

Distributed Robust Adaptive Frequency Regulation of Power Grid with Variable Renewable Integration

Hunmin Kim and Minghui Zhu

*The Department of Electrical Engineering and Computer Science
Pennsylvania State University
201 Old Main, University Park, PA, 16802*

Abstract

This paper investigates distributed angular frequency regulation of multi-machine power systems with wind generations when wind power signals' frequencies are known (and unknown). The challenge is to regulate angular frequencies under fast changing and unpredictable wind generations. To address the issue, we split unknown signals into three parts according to their frequency ranges and design an (adaptive) internal model to reconstruct the low and medium frequency parts. We integrate heterogeneous grid components to deal with fast changing signals. At each bus with wind power generations, a battery energy storage system is used to filter out high frequency components of wind generations. At generator bus, demand response is utilized to deal with their medium frequency components and a synchronous generator is exploited to handle their low frequency components. At load bus, demand response handles low and medium frequency components. The proposed controllers ensure exponential stability (and asymptotic convergence) of system states with respect to their desired signals. Simulations on the IEEE 68-bus test system are conducted to demonstrate the effectiveness of the proposed controllers.

1 Introduction

1.1 Motivation

Current power grid is being modernized into smart grid by enabling the integrations of advanced information and communication technologies relating power consumption and storage [4]. Integrating new technologies to power grid enables us to control the grid in a more flexible and efficient manner. For example, two-way communication and information technologies allow the use of demand response and automatic meter reading, respectively. Another important feature is to merge variable renewable energy sources such as wind, solar, and wave energy generators to the grid. It is well known that renewable energy attracts more attentions due to its cleanness and profitability. Worldwide 144 countries now have their own political targets for increasing shares of renewable energy generations and especially European Union targets 20% of renewable energy shares by 2020 [42].

However, variable renewable integration imposes challenges to operation and management of power grid. As pointed out in [5,37], renewable energy can not be fully predicted. There are many wind forecasting methods which are well surveyed in [13], but forecasting errors could be one source for uncertainties and become dominant as time horizon increases. Another source of uncertainties is the increasing use of intermittent renewable energy sources in a distributed way [28]. Even more it fluctuates fast and largely [18]. For example, wind power generation contains 0.5Hz high frequency components [5]. Fast changing generation of renewable energy with unknown amount of power threatens the stability of the power grid [15,49]. Furthermore, it is difficult for a synchronous generator to track fast changing signals because it has a high inertia.

1.2 Contribution

In this paper, we consider distributed frequency regulation problems in smart power grid with integration of wind power energy, demand response, and battery energy storage system (BESS). Designed distributed controllers are expected to regulate angular frequencies to a desired common constant under fast changing and unknown wind generations. In particular we study the following two problems. The first problem is *distributed robust frequency regulation* with known frequencies of

* Hunmin Kim and Minghui Zhu are with the Department of Electrical Engineering and Computer Science, Pennsylvania State University, 201 Old Main, University Park, PA, 16802
Email addresses: hunminkim3@gmail.com (Hunmin Kim), muz16@psu.edu (Minghui Zhu).

wind power generations. The known frequency assumption is relaxed in the second problem called *distributed robust adaptive frequency regulation*. We propose the distributed controllers with (adaptive) internal model. Under the proposed distributed controllers, mechanical generation and elastic load are able to completely reject unknown wind power generations, regulating network wide angular frequencies to a desired constant. To our best knowledge, there is no existing controller which achieves this performance when frequencies of wind power generations are unknown. Moreover, this paper is the first time to investigate distributed adaptive internal model control. Furthermore, we match the trackable frequencies of wind generations with different grid components to balance the power generations and demand. This idea is inspired by the fact that each controllers have different inertias and thus they have different ranges of trackable frequencies of signals.

We first split wind power generation signals into low, medium, and high frequency parts, which is based on Van der Hoven's horizontal wind speed spectrum model [56] and trigonometric function formulas. At each bus, a BESS is interconnected with wind power generations to filter out the high frequency parts. The low and medium components are asymptotically reconstructed via a local internal model. At generator bus, the reconstructed signals are tracked by two different controllers. Mechanical power generations track the low frequency parts and elastic demands are driven by real-time prices to track the medium frequency parts. At load bus, elastic demands track both the low and medium frequency parts of wind power.

The remaining part of our solution of each problem is described as follows.

Solution 1: Robust frequency regulation. We first convert the global frequency regulation problem into a global stabilization problem. The augmented system at each generator bus consists of synchronous generator, demand response, and internal model. The augmented system at each load bus consists of demand response, and internal model. They are in a lower triangular structure. In the same coordinate transformation, redundant terms inspired by back-stepping are added to stabilize the system from the outer state to inner state. The state of each augmented system becomes input to state stable (ISS) with respect to the states of neighboring augmented systems. We choose control gains such that state transition matrix be Hurwitz to stabilize the networked system. It has been shown that, even when each control authorities can access to their local parameters only, the stabilizing controllers can be designed always. In this case, the control gains are designed such that local ISS gain functions are contraction mappings. A newly derived distributed constrained small gain theorem ensures that the collection of local contraction mappings are sufficient for the network stability. Con-

sequently, the proposed distributed controllers with the local internal models ensure that all the states are exponentially stable with respect to the desired manifolds.

Solution 2: Robust adaptive frequency regulation. Designing an internal model requires a constant matrix which depends on frequencies of wind power generations. The frequencies of wind generations, however, are unknown and thus it is required to estimate the matrix. We design a projected adaptive parameter estimator for this purpose. We again solve the problem by converting the frequency regulation problem into a global stabilization problem with back-stepping inspired coordinate transformation terms to make the augmented system ISS with respect to the neighboring states. The proposed distributed controllers with adaptive internal model guarantee asymptotic convergence of all the states to their manifolds instead of exponential stability *Solution 1* can guarantee. Moreover, it is assumed that the synchronous generator model can be slightly simplified.

This paper is enriched from our preliminary results [23]. First of all, we relax the known frequency assumption; i.e., *Solution 2*. Secondly, we relax the assumption on the bus. Previously, we assume that each bus must have a generator and load. To make the problem more realistic, in this paper, we consider more types of buses as shown in Figure 1. Thirdly, simulations are applied to a more

Type	Synchronous generator	Load	Wind turbine
1	X	X	X
2	X	X	-
3	X	-	X
4	X	-	-
5	-	X	X
6	-	X	-
7	-	-	-

Fig. 1. List of bus types we consider

complex and realistic topology. Lastly, there are detailed proofs which were omitted from the preliminary results.

1.3 Literature review

Distributed control methods on power system have been studied extensively. Primary control (droop-control) scheme adjusts mechanical power generations to stabilize the frequencies via governors in a decentralized way [10,43]. To improve restoration of angular frequency, secondary control is introduced. Secondary control (automatic generation control) tunes the set-point of governors to achieve nominal frequencies in a centralized way [25,59]. Our control problems consider the primary and secondary controls at the same time in a distributed way under the existence of fast changing and unknown signals.

There have been attempts attenuating the impact of the uncertainties induced by renewable energy, power demand, and other sources. Robust control techniques include Riccati equation [29,41], H_2/H_∞ control [6,11,12,47], LMIs [33,48], etc. Also, it was shown that oscillations induced by load disturbances can be effectively alleviated by a BESS [16,20,30,61]. Another way to address the uncertainties is to reject disturbances and/or asymptotically track reference signals. Internal model has been widely used to achieve the goal [14,19,39,46]. On power systems, recent paper [8] uses internal model principle to address uncertainty induced by time varying demands. Different from our work, the paper [8] only deals with secondary control on a simpler (second order) model with voltage dynamics, and guarantees regional asymptotic convergence rate assuming that frequencies of demand signals are known. Only with the known frequency assumption, our first solution guarantees global exponential convergence of the fourth order dynamics. We further extend that, with unknown frequencies, our second solution guarantees global asymptotic convergence of the third order dynamics. On top of this, we split unknown signals into three parts according to their frequency ranges to be tracked and filtered by two different controllers and BESS.

Traditional approach to balance power demand and generation is to adjust power generations. Some of recent studies focus on achieving the power balance via demand controlling such as optimal load control [62], load switch [21], etc. The features and overview of demand side control is well introduced in [54]. It has been proposed that load side control can be faster and have a large capacity through implementing a switching device so that such control scheme is used to assist conventional mechanical generation system [31,45]. In this paper, real-time demand response is used to track medium (and low) frequency parts of wind power generations at generator bus (at load bus).

This paper is organized as follows. We start by introducing all the system models in Section 2. Based on the illustrated models, the two problems; i.e., *robust frequency regulation* and *robust adaptive frequency regulation* problems are described in Section 3. We propose solutions for the problems in Section 4 and 5, respectively. Stability is formally analyzed. Lastly, Section 6 presents simulations of frequency regulation on the IEEE 68-bus test system to illustrate the performance of our controllers.

1.4 Notation

We define $\|x\|_{[t_1, t_2]} \triangleq \sup_{t_1 \leq t \leq t_2} \|x(t)\|$. Matrix I_d denotes the identity matrix with dimension $d \times d$. $\text{diag}(A_1, \dots, A_n)$ denotes a block matrix having A_1 to A_n as main diagonal blocks and the off-diagonal blocks are all zero matrices. Notation $\vec{0}_n$ indicates the $1 \times n$

dimensional zero row vector. For a set \mathcal{S} , its cardinality is described by $|\mathcal{S}|$.

For a positive constant $\alpha > 0$ and a vector $B = [b_1, b_2, \dots, b_n]^T$, function $\text{sign}_\alpha : \mathbb{R}^n \rightarrow \mathbb{R}^n$ is defined by $\text{sign}_\alpha(B) \triangleq [\hat{b}_1, \hat{b}_2, \dots, \hat{b}_n]^T$ where, for $\forall i \in \{1, \dots, n\}$, $\hat{b}_i \triangleq 1, 0$ and -1 if $b_i \geq \alpha$, $|b_i| < \alpha$, and $b_i \leq -\alpha$, respectively. Frobenius norm is a vector norm defined by $\|A\|_F \triangleq \sqrt{\sum_{i=1}^n \sum_{j=1}^m |a_{ij}|^2}$ where a_{ij} is the i^{th} row and j^{th} column of matrix $A \in \mathbb{R}^{n \times m}$. We use 2 norm $\|\cdot\|_2$ if it is not specified.

The following definition of input-to-state stability is adopted from [51].

Definition 1.1 *The system $\dot{x} = f(x, u, t)$ is input-to-state stable (ISS) if there are a class \mathcal{KL} function β and a class \mathcal{K} function ξ such that for all $t \geq t_0$,*

$$\|x(t)\| \leq \beta(\|x(t_0)\|, t - t_0) + \xi(\|u\|_{[t_0, t]})$$

for any initial state $x(t_0)$ and any bounded input $u(t)$.

2 System Model

The present section introduces system models on which our problem based. We illustrate the models of power network, synchronous power generator, wind power, BESS, and demand response. To avoid notational confusion, we begin by introducing system variables and parameters as follows.

Table 1. System parameters

Generator variables			
w	angular frequency	θ	phase angle
P_M	mechanical power	P_L	actual load
P_v	steam valve position	P_{ref}	reference power
P_{ren}	actual turbine power	P_{ij}	power flow
Generator parameters			
D	load-damping constant	m	angular momentum
T_{CH}	charging time constant	t_{ij}	tie-line stiffness
T_G	governor time constant	R	feedback loop gain
Wind power system			
P_w	wind power	v	wind speed
ρ	air density	r	blade length
C_p	power coefficient		

2.1 Power network model

Power network is described by an undirected graph $(\mathcal{V}, \mathcal{E})$ where $\mathcal{V} \triangleq \{1, \dots, N\}$ denotes the set of buses in the network and $\mathcal{E} \subseteq \mathcal{V} \times \mathcal{V}$ denotes the set of transmission lines between buses. The set \mathcal{N}_i denotes the time invariant set of neighboring buses of $i \in \mathcal{V}$; i.e., $\mathcal{N}_i \triangleq \{j \in \mathcal{V} \setminus \{i\} | (i, j) \in \mathcal{E}\}$.

Each bus is either a generator bus $i \in \mathcal{G}$, load bus with nonzero load $i \in \mathcal{L}$ or load bus with zero load $i \in \mathcal{T}$ where \mathcal{G} , \mathcal{L} , and \mathcal{T} denote the set of corresponding buses. Buses $i \in \mathcal{G}, \mathcal{L}$ belong to a local control authority.

The generator bus consists of mechanical generation $P_{M_i}(t)$, wind power generation $P_{ren_i}(t)$, and load $P_{L_i}(t)$. The control authority $i \in \mathcal{G}$ can control mechanical generation via reference input and elastic load via power pricing. The load bus $i \in \mathcal{L}$ consists of wind power generation $P_{ren_i}(t)$, and load $P_{L_i}(t)$. The control authority $i \in \mathcal{L}$ can control elastic load via power pricing. The load bus $i \in \mathcal{T}$ does not belong to any control authority and its local system cannot be controlled.

Remark 2.1 Integrating consumer as a part of grid component via real time pricing can reduce the need for some infrastructures such as new power plants while maintaining the quality and reliability of electricity [36]. Integration of demand response as an auxiliary control method is suggested in [3, 62].

2.2 Generator and load bus dynamics

We adopt the fourth order model of synchronous power generator from [58] with integrating wind power generation signals $P_{ren_i}(t)$ as a negative load or a part of generation shown in [1, 27, 34, 60]. Consider, for $i \in \mathcal{G}$,

$$\begin{aligned} \dot{\theta}_i(t) &= 2\pi w_i(t) \\ \dot{w}_i(t) &= -\frac{1}{m_i} (D_i w_i(t) + \sum_{j \in \mathcal{N}_i} P_{ij}(t) - P_{M_i}(t) \\ &\quad + P_{L_i}(t) - P_{ren_i}(t)) \\ \dot{P}_{M_i}(t) &= -\frac{1}{T_{CH_i}} (P_{M_i}(t) - P_{v_i}(t)) \\ \dot{P}_{v_i}(t) &= -\frac{1}{T_{G_i}} (P_{v_i}(t) + \frac{1}{R_i} w_i(t) - P_{ref_i}(t)) \end{aligned} \quad (1)$$

where $P_{ij}(t) = t_{ij}(\theta_i(t) - \theta_j(t))$ and $\theta_i(t), \theta_j(t) \in [0, 2\pi)$. The first equation in (1) indicates the evolution of phase angle $\theta_i(t)$. The second equation is referred to as swing dynamics, indicating frequency fluctuations due to power imbalances. A general control objective is to regulate all the angular frequencies $w_i(t)$ to a constant set point w^* . To achieve this, it is required to balance the power generations and demand, otherwise frequency

$w_i(t)$ changes. For example, frequency $w_i(t)$ increases if the aggregate of power generation surpasses power demand $P_{M_i}(t) + P_{ren_i}(t) > \sum_{j \in \mathcal{N}_i} P_{ij}(t) + P_{L_i}(t)$, and decreases with a reversed inequality. The third and forth equations denote turbine governor dynamics with reference input $P_{ref_i}(t)$. Governor regulates torque of the rotor and eventually regulates angular frequency $w_i(t)$ to a desired set point w_i^* .

Remark 2.2 The fourth order synchronous generator model (1) can be simplified to the third order model [58]:

$$\begin{aligned} \dot{\theta}_i(t) &= 2\pi w_i(t) \\ \dot{w}_i(t) &= -\frac{1}{m_i} (D_i w_i(t) + \sum_{j \in \mathcal{N}_i} P_{ij}(t) - P_{M_i}(t) \\ &\quad + P_{L_i}(t) - P_{ren_i}(t)) \\ \dot{P}_{M_i}(t) &= -\frac{1}{T_{CH_i}} (P_{M_i}(t) - P_{v_i}(t)) \end{aligned} \quad (2)$$

where $P_{v_i}(t)$ is the input of this simplified system.

In the case of load bus $i \in \mathcal{L}$, the dynamic equation model can be expressed by the first and second differential equation of (1) with no mechanical generation $P_{M_i}(t) = 0$ as proposed in [17]:

$$\begin{aligned} \dot{\theta}_i(t) &= 2\pi w_i(t) \\ \dot{w}_i(t) &= -\frac{1}{m_i} (D_i w_i(t) + \sum_{j \in \mathcal{N}_i} P_{ij}(t) + P_{L_i}(t) - P_{ren_i}(t)) \end{aligned} \quad (3)$$

where, in this load bus model, values m_i and D_i are effective moment and damping constants of a postulated load model. The dynamic equation model of bus $i \in \mathcal{T}$ is also described by (3) with $P_{L_i}(t) = P_{ren_i}(t) = 0$.

2.3 Wind power model

As [27, 32, 55], consider the wind power generation system of control authority $i \in \mathcal{V}$ described by

$$P_{w_i}(t) = \frac{1}{2} \rho \pi r_i^2 v_i^3(t) \quad P'_{ren_i}(t) = C_{p_i} P_{w_i}(t) \quad (4)$$

where C_{p_i} denotes turbine's power coefficient and each wind power generator might have different coefficient. It is pointed out in [5, 37] that, due to unknown fluctuations of wind speed $v_i(t)$, wind power generation $P'_{ren_i}(t)$ cannot be fully predicted. Therefore, it is difficult to track the power imbalances caused by wind power fluctuations. To deal with this problem, we first divide wind power generations into three parts according their frequency ranges:

$$P'_{ren_i}(t) = P_{ren_i}^L(t) + P_{ren_i}^M(t) + P_{ren_i}^H(t) \quad (5)$$

where $P_{ren_i}^L(t)$, $P_{ren_i}^M(t)$, and $P_{ren_i}^H(t)$ denote low, medium, and high frequency parts of wind generations.

Remark 2.3 *The frequency partitioning is based on Van der Hoven's horizontal wind speed spectrum model [56] and trigonometric function formulas. There are many studies including [35,40,50] based on this wind speed spectrum model. According to the wind speed spectrum model, wind speed can be approximated well by a combination of sinusoidal functions. By applying trigonometric function formulas to the first equation in (4), we can also approximate wind power generations as a combination of sinusoidal functions. Considering dominant frequencies of wind speed: 0.01cycles/hour and 0.1cycles/hour, we suggest that approximate ranges are $0 \sim 1.0 \times 10^{-4} \text{rad}$ for low, $1.0 \times 10^{-4} \sim 1.0 \times 10^{-3} \text{rad}$ for medium, and all the higher ranges for high frequency generations. ■*

By Van der Hoven's wind speed spectrum model [56], we assume that $P_{ren_i}^L(t)$ and $P_{ren_i}^M(t)$ are generated by a partially known exosystem which is described by

$$\dot{\chi}_i(t) = \Phi_i \chi_i(t), \quad P_{ren_i}^L(t) + P_{ren_i}^M(t) = \Psi_i \chi_i(t) \quad (6)$$

where states $\chi_i(t) = [\chi_{i,1}^L(t), \dot{\chi}_{i,1}^L(t), \dots, \chi_{i,\ell^L}^L(t), \dot{\chi}_{i,\ell^L}^L(t), \chi_{i,1}^M(t), \dot{\chi}_{i,1}^M(t), \dots, \chi_{i,\ell^M}^M(t), \dot{\chi}_{i,\ell^M}^M(t)]^T \in \mathbb{R}^{2\ell}$ denote exogenous signals. Each state represents a sinusoidal signal. Values ℓ^L and ℓ^M denote the maximum number of low/medium frequency parts of wind power generations, and $\ell = \ell^L + \ell^M$. Matrix $\Phi_i(\rho_i)$ is defined by $\Phi_i(\rho_i) \triangleq \text{diag}(\Phi_{i,1}^L, \dots, \Phi_{i,\ell^L}^L, \Phi_{i,1}^M, \dots, \Phi_{i,\ell^M}^M)$ where

$$\Phi_{i,l}^L \triangleq \begin{bmatrix} 0 & 1 \\ -(\rho_{i,l}^L)^2 & 0 \end{bmatrix}, \quad \Phi_{i,l}^M \triangleq \begin{bmatrix} 0 & 1 \\ -(\rho_{i,l}^M)^2 & 0 \end{bmatrix}.$$

The values $\rho_{i,l}^L$ for $\forall l \in \{1, \dots, \ell^L\}$ and $\rho_{i,l}^M$ for $\forall l \in \{1, \dots, \ell^M\}$ denote low and medium frequencies, respectively. The dependency of Φ_i on ρ_i is emphasized where ρ_i is the set of all $\rho_{i,l}^L$ and $\rho_{i,l}^M$. In exosystem (6), $P_{ren_i}(t)$ is a linear combination of sinusoidal functions with frequencies $\rho_{i,l}^L$ and $\rho_{i,l}^M$. Frequencies could be zero, i.e., $\rho_{i,l}^L = \rho_{i,k}^M = 0$ for some l, k . For nonzero frequencies, it always holds that $\rho_{i,l}^L < \rho_{i,k}^M$ for $\forall l$ and $\forall k$ such that $\rho_{i,k}^M > 0$. For example, assume $\ell^L = \ell^M = 1$ and $\Psi_i = [0, 1, 1, 0]$. Exosystem generates $\chi_{i,1}^L(t) = a_i^L \sin(\rho_{i,1}^L(t - \xi_i^L))$ and $\chi_{i,1}^M(t) = a_i^M \sin(\rho_{i,1}^M(t - \xi_i^M))$ where a_i^L, a_i^M, ξ_i^L , and ξ_i^M are constants decided by initial conditions of (6). Then wind power generations are given by a combination of sinusoidal functions: $P_{ren_i}(t) = \dot{\chi}_{i,1}^L(t) + \chi_{i,1}^M(t) = a_i^L \rho_{i,1}^L \cos(\rho_{i,1}^L(t - \xi_i^L)) + a_i^M \sin(\rho_{i,1}^M(t - \xi_i^M))$.

The control authority i cannot measure exosystem states $\chi_i(t)$, and initial conditions $\chi_i(t_0)$. Frequencies $\rho_{i,l}$ are known in the first problem, and unknown in the second

problem. It implies that amplitudes and phase shifts of sinusoidal functions are unknown because they are determined by unknown initial conditions of (6). However, the structure of the exosystem and Ψ_i are known to the control authorities.

2.4 Battery energy storage system

We have proposed that wind power generation signals can be divided into low, medium and high frequency parts. However, synchronous generators and demand response cannot track fast changing high frequency wind power generations. To increase generation quality, it is proposed that a BESS can be used to smooth renewable energy fluctuations in [16,20,61]. To filter out $P_{ren_i}^H$, we place the BESS at the output of wind power generations. The BESS acts as a low pass filter; i.e., the signal loses its high frequency components $P_{ren_i}^H \simeq 0$ by going through the BESS. Consider the transfer function of the BESS, as [16,20,61],

$$P_{ren_i}(s) = \frac{1}{(1 + sT)} P'_{ren_i}(s) \quad (7)$$

where $P'_{ren_i}(s)$ and $P_{ren_i}(s)$ denote the Laplace transforms of the input and output power of the BESS, respectively. The effectiveness of transfer function (7) is determined by the time constant T . Therefore, it is important to choose a proper constant T such that the transfer function sufficiently suppresses the high frequency wind power generation $P_{ren_i}^H(t)$. With input (5), the output of the BESS is $P_{ren_i}(t) = P_{ren_i}^M(t) + P_{ren_i}^L(t)$.

2.5 Demand model

Local power demand $P_{L_i}(t)$ of bus $i \in \mathcal{G}, \mathcal{L}$ includes all the local power consumptions of consumers, instantaneous and aggregate demands. Demand $P_{L_i}(t)$ can be separated into elastic demand $P_{L_i}^E(t)$ and inelastic demand $P_{L_i}^{IE}(t)$ as shown in [2,3,9]; i.e., $P_{L_i}(t) = P_{L_i}^E(t) + P_{L_i}^{IE}(t)$. Under the assumption that marginal benefit function $b'_i + c'_i P_{L_i}^E(t)$ of consumer is negatively proportional to the power consumption, elastic demand $P_{L_i}^E(t)$ is governed by the following dynamics:

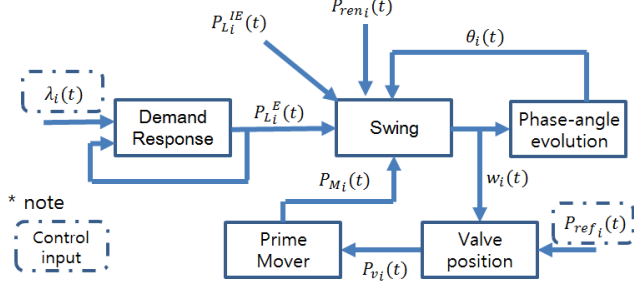
$$\dot{P}_{L_i}^E(t) = b_i + c_i P_{L_i}^E(t) - \lambda_i(t) \quad (8)$$

where $b_i = \frac{b'_i}{\tau_i}$, $c_i = \frac{c'_i}{\tau_i}$, $\lambda_i(t) = \frac{\lambda'_i(t)}{\tau_i} \in \mathbb{R}$. Parameters b'_i and c'_i denote power consumer benefits and τ_i is a consumer response constant. Real-time electricity price $\lambda'_i(t)$ can be used as a controller. In (8), the power demand would increase when marginal benefit is greater than the given price $\lambda'_i(t)$. The way to choose parameters b'_i and c'_i , and constant τ_i is introduced in [3]. For notational simplicity, we introduce pricing controller $\lambda_i(t)$ instead of $\lambda'_i(t)$. We assume that time varying inelastic

power demand $P_{L_i}^{IE}(t)$, and constants b_i, c_i are known to control authority i .

2.6 Discussion

Generator Bus



Load Bus

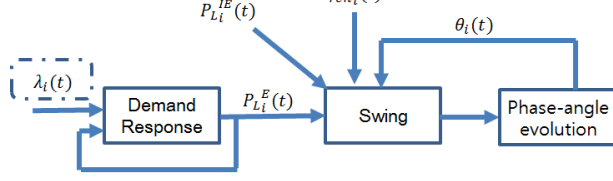


Fig. 2. Block diagrams of generator $i \in \mathcal{G}$ and load bus $i \in \mathcal{L}$

All the power generations and loads are coupled via swing dynamics, the second equation of (1). The schematic connections are described in Figure 2. At generator bus, reference power $P_{ref_i}(t)$ and pricing control $\lambda_i(t)$ are control inputs available to the local control authority. All the states in the diagram are used to determine inputs (state feedback control) and the control authorities' objective is to regulate all the states to desired manifolds. At load bus $i \in \mathcal{L}$, available control input is pricing control $\lambda_i(t)$ only.

In our system setting, wind power generations are allowed to be zero for any bus. Therefore, each bus has a freedom to remove the wind power system with the BESS. This implies that the system without wind power generators is a special case of the wind power integrated system. Moreover, if medium frequency parts of wind power generations at a generator bus are missing, then demand response can also be removed at the same bus because the role of demand response at the generator bus is only to follow medium frequency wind generation.

3 Problem statements and preliminaries

We consider two frequency regulation problems. Both problems aim to regulate angular frequencies to a constant and phase angle differences between neighboring buses to specified constants. In the first problem illustrated in Section 3.1, we assume that frequencies of wind power generation signals are known to control authorities. This assumption is relaxed in the second problem

in Section 3.2. In the second problem, it is only assumed that the maximum number of frequencies is known. As a preliminary step to solve the two problems, a local internal model is designed in Section 3.3 to reconstruct unknown wind power generations.

3.1 Problem statement 1: Robust frequency regulation.

Our objective is to regulate frequency $w_i(t)$ to a desired constant w^* ; e.g., 60Hz, and $\theta_i(t)$ to $\theta_i^*(t) = 2\pi w^*t + \theta_i^{**}$ under unpredictable wind generations. Constant phase shift θ_i^{**} could be different from θ_j^{**} for $i \neq j$.

In the generator bus, to achieve this goal, $P_{M_i}(t)$ is expected to track low frequency wind power generation $P_{ren_i}^L(t)$ via input $P_{ref_i}(t)$ and $P_{L_i}^E(t)$ is expected to track medium frequency wind power generation $P_{ren_i}^M(t)$ via pricing control $\lambda_i(t)$. By examining all the system models described in Section 2, we have desired states and inputs which are called manifolds:

$$\begin{aligned} \theta_i^*(t) &= 2\pi w^*t + \theta_i^{**}, \quad w_i^* = w^*, \quad P_{L_i}^E(t) = P_{ren_i}^M(t) \\ P_{M_i}^*(t) &= P_{L_i}^{IE}(t) - P_{ren_i}^L(t) + D_i w^* + \sum_{j \in \mathcal{N}_i} P_{ij}^* \\ P_{v_i}^*(t) &= T_{CH_i}(\dot{P}_{L_i}^{IE}(t) - \dot{P}_{ren_i}^L(t)) + P_{L_i}^{IE}(t) \\ &\quad - P_{ren_i}^L(t) + D_i w^* + \sum_{j \in \mathcal{N}_i} P_{ij}^* \\ P_{ref_i}^*(t) &= T_{G_i} T_{CH_i}(\ddot{P}_{L_i}^{IE}(t) - \ddot{P}_{ren_i}^L(t)) \\ &\quad + (T_{G_i} + T_{CH_i})(\dot{P}_{L_i}^{IE}(t) - \dot{P}_{ren_i}^L(t)) \\ &\quad + P_{L_i}^{IE}(t) - P_{ren_i}^L(t) + (D_i + \frac{1}{R})w^* + \sum_{j \in \mathcal{N}_i} P_{ij}^* \\ \lambda_i^*(t) &= -\dot{P}_{ren_i}^M(t) + c_i P_{ren_i}^M(t) + b_i \end{aligned} \quad (9)$$

where $P_{ij}^* = t_{ij}(\theta_i^{**} - \theta_j^{**})$. It is emphasized that manifolds $x_i^*(P_{ren_i}(t), t) \triangleq [\theta_i^*(t), w_i(t), P_{M_i}^*(t), P_{v_i}^*(t), P_{L_i}^E(t)]^T$ and $u_i^*(P_{ren_i}(t), t) \triangleq [P_{ref_i}^*(t), \lambda_i^*(t)]$ are functions of unknown wind power energy $P_{ren_i}^L(t)$ and $P_{ren_i}^M(t)$. To ensure the existence of the manifold (9), we have Assumptions 3.1 and 3.2.

Assumption 3.1 Inelastic power demand $P_{L_i}^{IE}(t)$ is a twice differentiable function for $\forall i \in \mathcal{V}$.

Assumption 3.2 For the set of desired power flow P_{ij}^* for $\forall (i, j) \in \mathcal{E}$, there exists a set of solutions θ_i^{**} and θ_j^{**} for equation $P_{ij}^* = t_{ij}(\theta_i^{**} - \theta_j^{**})$. For all the buses $i \in \mathcal{T}$, desired incoming and outgoing power flows are balanced; i.e., $\sum_{j \in \mathcal{N}_i} P_{ij}^* = 0$ for $i \in \mathcal{T}$.

We desire to design distributed controllers which regulate the system states $x_i'(t) = [x_{i,1}(t), x_{i,2}(t), x_{i,3}(t), x_{i,4}(t), x_{i,5}(t)]^T \triangleq [\theta_i(t), w_i(t), P_{M_i}(t), P_{v_i}(t),$

$P_{L_i}^E(t)]^T$ and inputs $u_i(t) \triangleq [P_{ref_i}(t), \lambda_i(t)]^T$ to their manifolds $x_i^{*'}(P_{ren_i}(t)(t), t)$ and $u_i^*(P_{ren_i}(t), t)$ exponentially for $\forall i \in \mathcal{G}$. However, it is challenged by the fact that exosystem states $\chi_i(t)$, and wind power generations $P_{ren_i}^L(t)$ and $P_{ren_i}^M(t)$ can not be directly measured. Hence, manifolds (9) are not measurable neither. To address the challenge, we will design local internal models to reconstruct (9) via state and input measurements. In this problem, we assume that all the frequencies of wind power generation signals are known to control authorities.

Assumption 3.3 *All the frequencies $\rho_{i,l}$ for $\forall l \in \{1, \dots, \ell\}$ of wind power generations $P_{ren_i}(t)$ are known to the local control authority i .*

In the load bus $i \in \mathcal{L}$, elastic demand $P_{L_i}^E$ is expected to track both low and medium frequency wind power generation and stabilize the frequency. Therefore, the manifolds for states $\theta_i(t)$ and $w_i(t)$ are identical to those of (9) but the manifold for the elastic demand $P_{L_i}^E(t)$ is $P_{L_i}^{E*}(t) - P_{M_i}^*(t)$ in (9). We desire to design distributed controllers which regulate the system states $x_i'(t) = [x_{i,1}(t), x_{i,2}(t), x_{i,3}(t)]^T \triangleq [\theta_i(t), w_i(t), P_{L_i}^E(t)]^T$ and inputs $u_i(t) \triangleq \lambda_i(t)$ to their manifolds $x_i^{*'}(P_{ren_i}(t)(t), t) = [\theta_i^*(t), w_i^*, -P_{M_i}^*(t) + P_{L_i}^{E*}(t)]^T$ and $u_i^*(P_{ren_i}(t), t) = -\dot{P}_{ren_i}(t) + \dot{P}_{L_i}^{IE}(t) + b_i + c_i(P_{ren_i}(t) - P_{L_i}^{IE} - D_i w_i^* - \sum_{j \in \mathcal{N}_i} P_{ij}^*)$ exponentially for $\forall i \in \mathcal{L}$.

3.2 Problem statement 2: Robust adaptive frequency regulation.

The objective of *Problem 2* remains the same as that of *Problem 1* but there are a couple of distinctions. First, control authorities do not know the frequencies of wind power generation signals in this problem; i.e., Assumption 3.3 is relaxed. Secondly, to solve this problem, we use the simplified synchronous generator model (2) and suppose that the following is true:

Assumption 3.4 *The control authorities know the maximum number ℓ^L, ℓ^M of low/medium frequency parts of wind power generations.*

Moreover, we assume that maximum frequency ρ_{\max} such that $\rho_{i,l}^L, \rho_{i,l}^M \leq \rho_{\max}$ for $\forall l$ is known because it can be estimated by the chosen time constant T .

In the generator bus, with the third order synchronous generator model (2), we have the same manifolds with (9) excluding $P_{ref_i}(t)$. Distributed controllers are expected to regulate the system states $x_i'(t) = [x_{i,1}(t), x_{i,2}(t), x_{i,3}(t), x_{i,4}(t)]^T \triangleq [\theta_i(t), w_i(t), P_{M_i}(t), P_{L_i}^E(t)]^T$ and inputs $u_i(t) \triangleq [P_{v_i}(t), \lambda_i(t)]^T$ to their manifolds $x_i^{*'}(P_{ren_i}(t), t)$ and $u_i^*(P_{ren_i}(t), t)$ asymptotically for $\forall i \in \mathcal{G}$.

In the load bus $i \in \mathcal{L}$, we desire to design distributed controllers which regulate the system states $x_i'(t) = [x_{i,1}(t), x_{i,2}(t), x_{i,3}(t)]^T \triangleq [\theta_i(t), w_i(t), P_{L_i}^E(t)]^T$ and inputs $u_i(t) \triangleq \lambda_i(t)$ to their manifolds $x_i^{*'}(P_{ren_i}(t), t) \triangleq [\theta_i^*(t), w_i^*, -P_{M_i}^*(t) + P_{L_i}^{E*}(t)]^T$ and $u_i^*(P_{ren_i}(t), t) = -\dot{P}_{ren_i}(t) + \dot{P}_{L_i}^{IE}(t) + b_i + c_i(P_{ren_i}(t) - P_{L_i}^{IE} - D_i w_i^* - \sum_{j \in \mathcal{N}_i} P_{ij}^*)$ asymptotically for $\forall i \in \mathcal{L}$.

3.3 Local internal models

To design a local internal model, we combine the third and fourth equations in (9):

$$\begin{aligned} & -P_{M_i}^*(t) + P_{L_i}^{E*}(t) + P_{L_i}^{IE}(t) + \sum_{j \in \mathcal{N}_i} P_{ij}^* + D_i w_i^* \\ & = P_{ren_i}^L(t) + P_{ren_i}^M(t) = \Psi_i \chi_i(t). \end{aligned} \quad (10)$$

Assumption 3.5 *The pair $(\Psi_i, \Phi_i(\rho_i))$ is observable for $\forall i \in \mathcal{V}$.*

Under Assumption 3.5, for any controllable pair (M_i, N_i) with $M_i \in \mathbb{R}^{2\ell \times 2\ell}$ being Hurwitz for $i \in \mathcal{V}$ and $N_i \in \mathbb{R}^{2\ell}$, there exists a unique non-singular matrix $T_i^*(\rho_i) \in \mathbb{R}^{2\ell \times 2\ell}$ for the Sylvester equation [7]:

$$T_i^*(\rho_i)\Phi_i(\rho_i) - M_i T_i^*(\rho_i) = N_i \Psi_i. \quad (11)$$

With $\vartheta_i(t) \triangleq T_i^*(\rho_i)\chi_i(t)$, (10) becomes

$$\begin{aligned} \Psi_i T_i^*(\rho_i)^{-1} \vartheta_i(t) &= -P_{M_i}^*(t) + P_{L_i}^{E*}(t) + P_{L_i}^{IE}(t) \\ &+ \sum_{j \in \mathcal{N}_i} P_{ij}^* + D_i w_i^*. \end{aligned}$$

Now we have a local internal model candidate:

$$\begin{aligned} \dot{\eta}_i(t) &= M_i \eta_i(t) + N_i (-P_{M_i}^*(t) + P_{L_i}^{E*}(t) + P_{L_i}^{IE}(t) \\ &+ \sum_{j \in \mathcal{N}_i} P_{ij}^* + D_i w_i^*), \quad \forall i \in \mathcal{G} \\ \dot{\eta}_i(t) &= M_i \eta_i(t) + N_i (P_{L_i}^{E*}(t) + P_{L_i}^{IE}(t) \\ &+ \sum_{j \in \mathcal{N}_i} P_{ij}^* + D_i w_i^*), \quad \forall i \in \mathcal{L} \end{aligned} \quad (12)$$

where $\eta_i(t) \in \mathbb{R}^{2\ell}$. Internal model (12) acts as an estimator and its states $\eta_i(t)$ are expected to asymptotically track unmeasurable states $\vartheta_i(t)$. The manifolds of internal model states $\eta_i(t)$ are $\eta_i^*(t) = \vartheta_i(t)$ in this case. Suitable controllers are able to stabilize error dynamics $\eta_i(t) - \vartheta_i(t)$. According to certainty equivalence principle [57], internal model states $\eta_i(t)$ are used to replace $\vartheta_i(t)$ in the manifolds so that the manifolds can be used in feedback control.

We want to estimate $P_{ren_i}^L(t)$ and $P_{ren_i}^M(t)$ separately. It is possible because $P_{ren_i}^L(t)$ and $P_{ren_i}^M(t)$ do not share the common frequencies $\rho_{i,l}$ and/or exosystem states $\chi_{i,l}(t)$. We define $\Psi_{i,1} \triangleq [\Psi_i^L, \vec{0}_{\ell^M}]$ and $\Psi_{i,2} \triangleq [\vec{0}_{\ell^L}, \Psi_i^M]$ where $\Psi_i \triangleq [\Psi_i^L, \Psi_i^M]$. Then $\Psi_{i,1} + \Psi_{i,2} = \Psi_i$, $P_{ren_i}^L = \Psi_{i,1} T_i^*(\rho_i)^{-1} \vartheta_i(t)$ and $P_{ren_i}^M = \Psi_{i,2} T_i^*(\rho_i)^{-1} \vartheta_i(t)$.

For notional simplicity, we will use states with internal model states $x_i(t) \triangleq [x_i^T(t), \eta_i^T(t)]^T$ and manifolds $x_i^*(P_{ren_i}(t), t) \triangleq [x_i^{*T}(P_{ren_i}(t), t), \vartheta_i^T(t)]^T$.

4 Solution 1: Robust frequency regulation

In this section, we present a solution of the *robust frequency regulation* problem described in Section 3.1. Under Assumptions 3.1, 3.2, 3.3, and 3.5, we design distributed controllers such that all the states are exponentially stable with respect to their manifolds.

In Section 4.1, we convert the frequency regulation problem into a stabilization problem. The resulting system is ISS with respect to neighboring states. In Section 4.2, we formally analyze the global exponential stability.

4.1 Coordinate transformation

The purpose of the coordinate transformation is to transform the global frequency regulation problem to manifolds (9) into the global stabilization problem. This can be done by subtracting manifolds (9) from the state and input variables.

To ensure the stability of the augmented system, we make use of its special lower triangular structural. It is possible to progressively stabilize from the outer state to the inner state. Therefore, we add more terms to the coordinate transformation inspired by backstepping [24] to guarantee stability.

Since internal model states $\eta_i(t)$ are expected to track $\vartheta_i(t)$ exponentially for $\forall i \in \mathcal{V}$, the estimation errors $\|\Psi_{i,j} T_i^*(\rho_i)^{-1} \eta_i(t) - \Psi_{i,j} T_i^*(\rho_i)^{-1} \vartheta_i(t)\|$ for $\forall j \in \{1, 2\}$ converge to zero exponentially. By certainty equivalent principle, we use the known term $\Psi_{i,j} T_i^*(\rho_i)^{-1} \eta_i(t)$ to replace unknown $\Psi_{i,j} T_i^*(\rho_i)^{-1} \vartheta_i(t)$ when subtracting the manifolds from the states. Consider the coordinate transformation described by

$$\hat{x}_i(t) \triangleq x_i(t) - x_i^*(\Psi_i T_i^*(\rho_i)^{-1} \eta_i(t), t) - \hat{x}_i^*(t) \quad (13)$$

where $\hat{x}_i^*(t) = [0, \hat{x}_{i,2}^*(t), \hat{x}_{i,3}^*(t), \hat{x}_{i,4}^*(t), 0, \hat{x}_{i,6}^*(t)]^T$ for $\forall i \in \mathcal{G}$, $\hat{x}_i^*(t) = [0, \hat{x}_{i,2}^*(t), -\hat{x}_{i,3}^*(t), \hat{x}_{i,6}^*(t)]^T$ for $\forall i \in \mathcal{L}$,

$\hat{x}_i^*(t) = [0, 0]^T$ for $i \in \mathcal{T}$ and

$$\begin{aligned} \hat{x}_{i,2}^*(t) &\triangleq -\frac{k_{i,1}}{2\pi} \hat{x}_{i,1}(t) \\ \hat{x}_{i,3}^*(t) &\triangleq \left(\sum_{k \in \mathcal{N}_i} t_{ij} - \frac{k_{i,1}}{2\pi} (D_i - m_i \Psi_i T_i^*(\rho_i)^{-1} N_i \right. \\ &\quad \left. - m_i k_{i,1}) \right) \hat{x}_{i,1}(t) + (D_i - m_i \Psi_i T_i^*(\rho_i)^{-1} N_i \\ &\quad - m_i k_{i,1} - m_i k_{i,2}) \hat{x}_{i,2}(t) \\ &\triangleq e_{M_{i,1}} \hat{x}_{i,1}(t) + e_{M_{i,2}} \hat{x}_{i,2}(t) \\ \hat{x}_{i,4}^*(t) &\triangleq e_{M_{i,1}} (1 - T_{CH_i} k_{i,1}) \hat{x}_{i,1}(t) \\ &\quad + (2\pi T_{CH_i} e_{M_{i,1}} + e_{M_{i,2}} - T_{CH_i} k_{i,2} e_{M_{i,2}}) \hat{x}_{i,2}(t) \\ &\quad + \left(1 + \frac{e_{M_{i,2}}}{m_i} T_{CH_i} - T_{CH_i} k_{i,3}\right) \hat{x}_{i,3}(t) \\ &\triangleq e_{v_{i,1}} \hat{x}_{i,1}(t) + e_{v_{i,2}} \hat{x}_{i,2}(t) + e_{v_{i,3}} \hat{x}_{i,3}(t) \\ \hat{x}_{i,6}^*(t) &\triangleq -m_i N_i (\hat{x}_{i,2}(t) - \frac{k_{i,1}}{2\pi} \hat{x}_{i,1}(t)) \end{aligned} \quad (14)$$

for arbitrary positive constants $k_{i,l}$ for $l \in \{1, 2, 3, 4\}$. Under coordinate transformation (13), our frequency regulation problem becomes the stabilization problem of all the transformed states. This is because states $x_i(t)$ converge to their manifolds if the system states $\hat{x}_i(t)$ and internal model state $\hat{\eta}_i(t)$ are stable. Note that additional coordinate transformation term $\hat{x}_i^*(t)$ does not change the origin.

Moreover, we choose a controller

$$u_i(t) = u_i^*(\Psi_i T_i^*(\rho_i)^{-1} \eta_i(t), t) + \hat{u}_i^*(t) \quad (15)$$

where $\hat{u}_i^*(t) = [\hat{P}_{ref_i}^*(t), \hat{\lambda}_i^*(t)]^T$ for $\forall i \in \mathcal{G}$, $\hat{u}_i^*(t) = \hat{\lambda}_i^*(t) = -e_{M_{i,1}} (c_i + k_{i,1}) \hat{x}_{i,1}(t) + (2\pi e_{M_{i,1}} - e_{M_{i,2}} (c_i + k_{i,2})) \hat{x}_{i,2}(t) + (c_i + k_{i,3} - \frac{e_{M_{i,2}}}{m_i}) \hat{x}_{i,3}(t)$ for $\forall i \in \mathcal{L}$ and

$$\begin{aligned} \hat{P}_{ref_i}^*(t) &= (e_{v_{i,1}} - \frac{k_{i,1}}{2\pi R_i} - T_{G_i} k_{i,1} e_{v_{i,1}}) \hat{x}_{i,1}(t) \\ &\quad + (e_{v_{i,2}} + \frac{1}{R_i} + 2\pi T_{G_i} e_{v_{i,1}} - T_{G_i} k_{i,2} e_{v_{i,2}}) \hat{x}_{i,2}(t) \\ &\quad + (e_{v_{i,3}} + \frac{T_{G_i}}{m_i} e_{v_{i,2}} - T_{G_i} k_{i,3} e_{v_{i,3}}) \hat{x}_{i,3}(t) \\ &\quad + (-T_{G_i} k_{i,4} + 1 + \frac{T_{G_i}}{T_{CH_i}} e_{v_{i,3}}) \hat{x}_{i,4}(t) \\ \hat{\lambda}_i^*(t) &= (c_i + k_{i,5}) \hat{x}_{i,5}(t) \end{aligned}$$

for a positive constant $k_{i,5}$. Through coordinate transformation (13) and input (15), system (1) and (8) and internal model (12) become

$$\begin{aligned} \dot{\hat{x}}_{i,l}(t) &= -k_{i,l} \hat{x}_{i,l}(t) + B_{i,l} \hat{x}_i(t) + \sum_{j \in \mathcal{N}_i} B_{ij,l} \hat{x}_j(t) \\ \dot{\hat{x}}_{i,6}(t) &= M_i \hat{x}_{i,6}(t) + B_{i,6} \hat{x}_i(t) + \sum_{j \in \mathcal{N}_i} B_{ij,6} \hat{x}_j(t) \end{aligned} \quad (16)$$

where $B_{i,l}$, and $B_{ij,l}$ are corresponding constant matrices.

The exponential stability of $\hat{x}_i(t)$ implies that the original system states and internal model $x_i(t)$, and inputs $u_i(t)$ in (1), (8), and (12) exponentially follow their manifolds (9) and $\vartheta_i(t)$. This is because the additional terms described in (14) are identical to zero when states $\hat{x}_i(t)$ are zero.

4.2 Frequency regulation analysis

The following theorem summarizes the exponential stability of system (1) with respect to its manifold (9). Consider Algorithm 1 with

$$e_{\eta_{i,1}} = (\frac{m_i k_{i,1}}{2\pi} M_i + (\frac{D_i k_{i,1}}{2\pi} + \sum_{j \in \mathcal{N}_i} t_{ij}) I_{2\ell}) N_i$$

$$e_{\eta_{i,2}} = -(m_i M_i + D_i I_{2\ell}) N_i, \quad e_{\eta_{i,3}} = N_i \sum_{j \in \mathcal{N}_i} t_{ij}.$$

Algorithm 1 Control gain designs

- 1: Choose $\delta > 0$;
 - 2: **for** $i \in \mathcal{V}$ **do**
 - 3: $k_{i,1} = 10\pi + \delta$;
 - 4: Choose a controllable pair $(M_i, \frac{C_i}{\|C_i\|})$;
 - 5: $\alpha_i = -\frac{\lambda_{\max}(M_i)}{1+\delta} \min_{l=1,2,3} \{ \frac{0.2}{\|e_{\eta_{i,l}}\|} \}$, $N_i = \alpha_i \frac{C_i}{\|C_i\|}$;
 - 6: Find the solution T_i of Sylvester equation (11).
 - 7: $k_{i,2} = \frac{5}{m_i} \max \{ \sum_{j \in \mathcal{N}_i} t_{ij}, 1, \|\Psi_i T_i^* (\rho_i)^{-1}\| \} +$
 δ ; $k_{i,3} = 5 \max \{ \frac{\|e_{M_{i,2}}\| \sum_{j \in \mathcal{N}_i} t_{ij}}{m_i}, \frac{\|e_{M_{i,2}}\|}{m_i}, \frac{1}{T_{CH_i}},$
 $\frac{\|e_{M_{i,2}} \Psi_i T_i^* (\rho_i)^{-1}\|}{m_i} \} + \delta$;
 - 8: (for $i \in \mathcal{G}$) $k_{i,4} = 5 \max \{ \|\frac{1}{m_i} (e_{v_{i,2}} -$
 $e_{M_{i,2}} e_{v_{i,3}})\| (1 + \sum_{j \in \mathcal{N}_i} t_{ij}), \|\frac{1}{m_i} (e_{v_{i,2}} -$
 $e_{M_{i,2}} e_{v_{i,3}}) \Psi_i T_i^* (\rho_i)^{-1}\| \} + \delta$; $k_{i,5} > 0$.
 - 9: **end for**
-

Theorem 4.1 *Under Assumptions 3.1, 3.2, 3.3, 3.5 and that (M_i, N_i) is controllable for $\forall i$, we apply distributed controllers (15) with internal model (12) to system (1). Then, states with internal model $x_i(t)$, and inputs $u_i(t)$ described in (1), (8), and (12) for $i \in \mathcal{V}$ are globally exponentially stable with respect to their manifolds (9) and $\vartheta_i(t)$ for any initial states $x_i(t_0)$ if and only if control gains $k_{i,k}$ and matrices M_i and N_i are chosen such that matrix \mathbf{A} is Hurwitz where $\hat{\mathbf{x}}(t) = \mathbf{A}\hat{\mathbf{x}}(t)$ and $\hat{\mathbf{x}}(t) = [\hat{x}_{i_1}^T(t), \hat{x}_{i_2}^T(t), \dots, \hat{x}_{i_N}^T(t)]^T$. Moreover, such control gains $k_{i,l}$ and matrices M_i and N_i always exist if $D_i > \sum_{j \in \mathcal{N}_i} t_{ij}$ for $\forall i \in \mathcal{T}$.*

PROOF. Sufficiency: Assume that \mathbf{A} is Hurwitz. Then, linear time invariance system $\hat{\mathbf{x}}(t) = \mathbf{A}\hat{\mathbf{x}}(t)$ in (16)

is exponentially stable. If $\hat{\mathbf{x}}$ is exponentially stable, then $\mathbf{x}(t)$ in (1) is exponentially stable with respect to their manifolds (9) and $\vartheta_i(t)$ because coordinate transformation \hat{x}_i^* in (13) does not change the origin.

Necessity: This can be proven by reversing the argument steps above.

Now we prove the existence of control gains and matrices by construction. Especially, one can always choose them via Algorithm 1.

We first show that Algorithm 1 always generates a set of control gains $k_{i,l}$ and matrices M_i, N_i . In the generator bus, since the selections of $k_{i,1}$ and M_i do not depend on $\alpha_i, k_{i,2}, k_{i,3}, k_{i,4}$, or $k_{i,5}$, we can freely choose $k_{i,1}$ and M_i through step 3 and 4 in Algorithm 1. After that, we can choose α_i because the selection of α_i does not depend on $k_{i,2}, k_{i,3}, k_{i,4}$, or $k_{i,5}$. Likewise, $k_{i,2}, k_{i,3}, k_{i,4}$, and $k_{i,5}$ can be chosen sequentially. For the load bus $i \in \mathcal{L}$, it can be proven with the same argument of the generator bus. This completes the proof.

We prove that matrix \mathbf{A} is Hurwitz by showing equivalent condition that is the exponential stability of states and internal model states. Assume that we apply the distributed controllers (15) and choose a set of control gains and matrices through Algorithm 1, and $D_i > \sum_{j \in \mathcal{N}_i} t_{ij}$ for $\forall i \in \mathcal{T}$.

First consider any $i \in \mathcal{G}, \mathcal{L}$ and choose quadratic Lyapunov function candidates as described by

$$V_{i,l}(t) \triangleq \frac{1}{2} \hat{x}_{i,l}^T(t) \hat{x}_{i,l}(t).$$

The Lie derivative of each Lyapunov function candidate along the trajectories of system (16) becomes

$$\dot{V}_{i,l}(t) = -k_{i,l} \hat{x}_{i,l}^2(t) + \hat{x}_{i,l} (B_{i,l} \hat{x}_i(t) + \sum_{j \in \mathcal{N}_i} B_{ij,l} \hat{x}_j(t)),$$

$$\dot{V}_{i,6}(t) = \hat{x}_{i,6}^T M_i \hat{x}_{i,6} + \hat{x}_{i,6}^T (B_{i,6} \hat{x}_i(t) + \sum_{j \in \mathcal{N}_i} B_{ij,6} \hat{x}_j(t)).$$

Note that Lyapunov candidate $V_{i,l}$ is ISS Lyapunov function [52] and there exists an ISS Lyapunov function if and only if the system is ISS (Theorem 1 in [52]). Therefore, this is equivalent to ISS with respect to neighboring states:

$$\|\hat{x}_{i,l}(t)\| \leq \max \{ e^{-k_{i,l} a_{i,l}(t-t_0)} \|\hat{x}_{i,l}(t_0)\|, \max_{k \neq l} \{ \gamma_{i,l,k}(k_{i,1}, \dots, k_{i,6}) \|\hat{x}_{i,k}\|_{[t_0, t]} \} \} \quad (17)$$

for $0 < a_{i,l} \leq 1$ and $k_{i,6} \triangleq \lambda_{\max}(M_i)$. We omit the expression of the ISS gains $\gamma_{i,l,k}$. Please refer Lemma 2.14 in [52] to get them. It is not difficult to show that the

chosen control gains satisfy $0 \leq \gamma_{i,l,k}(k_{i,1}, \dots, k_{i,6}) < 1$; ISS contraction gain mappings.

Now consider any bus $i \in \mathcal{T}$. With $k_{i,1} = 0$, eigenvalues of local system $i \in \mathcal{T}$ are the solutions of

$$\lambda^2 + \frac{D_i}{m_i} \lambda + \frac{2\pi \sum_{j \in \mathcal{N}_i} t_{ij}}{m_i} = 0.$$

This implies that all the eigenvalues λ have negative real parts because $\frac{D_i}{m_i} > 0$ and $\frac{2\pi \sum_{j \in \mathcal{N}_i} t_{ij}}{m_i} > 0$; the local system is ISS with respect to neighboring states. Its ISS gain functions are, for $\forall k \in \mathcal{N}_i$, $\gamma_{i,2,k} = \frac{\sum_{j \in \mathcal{N}_i} t_{ij}}{\alpha D_i} < 1$ where $\alpha \simeq 1$ but $\alpha < 1$; ISS contraction gain mappings.

All the ISS gains $\gamma_{i,l,k}(\cdot)$ are contraction mappings. By distributed constrained small gain theorem 7.1 in Appendix, we can ensure the stability of the given systems. Moreover, by Remark 7.1, (17) ensures the exponential stability of $\hat{x}_i(t)$. This implies that \mathbf{A} is Hurwitz. ■

In Theorem 4.1, we show the sufficient and necessary condition of distributed controllers which ensure the global exponential stability of $\hat{x}_i(t)$ as well as the global exponential stability of $x_i(t)$ with respect to their manifolds. The stability of $x_i(t)$ implies that inputs $u_i(t)$ converge to their manifolds. However, to guarantee matrix \mathbf{A} is Hurwitz, all the network-wide system information need to be known. Moreover, all of the new controllers should be redesigned whenever there is a new integration, change or detachment of a grid component.

Algorithm 1 shows another extreme; when only local system information is available to each control authorities, still it is always possible for them to design distributed controllers such that matrix \mathbf{A} is Hurwitz, or equivalently, the system with internal model (12) is exponentially stable. It is not difficult to check that Algorithm 1 requires local information only. If the control gains and matrices are chosen through Algorithm 1, only local control gains should be modified when there is parameter changes because control gains and matrices depend on their local information only.

It should be emphasized that there is a trade off between parameter information and conservativeness. Algorithm 1 requires local information only, but it might result in conservative control gains and matrices.

The controller design in this section bases on Assumption 3.3; i.e., all the frequencies of wind power generation signals are known. If this is the case, control authorities can directly access the solution $T_i^*(\rho_i)$ of Sylvester equation and thus, controllers can use the terms $\Psi_{i,1}T_i^*(\rho_i)^{-1}\eta_i(t)$ and $\Psi_{i,2}T_i^*(\rho_i)^{-1}\eta_i(t)$ to estimate unknown terms. However, if this is not the case,

the control authorities can not access the term $T_i^*(\rho_i)^{-1}$ and thus term $\Psi_{i,l}T_i^*(\rho_i)^{-1}\eta_i(t)$ cannot be part of manifolds or coordinate transformation. We deal with this problem in Section 5.

5 Solution 2: Robust adaptive frequency regulation

In this section, we consider the case that control authority i cannot directly access true value $T_i^*(\rho_i)^{-1}$ which depends on unknown frequencies ρ_i . For this reason, we adopt an adaptive technique for $\Psi_i T_i^{-1}(t)$ to asymptotically reconstruct the true value $\Psi_i T_i^*(\rho_i)^{-1}$ where $T_i^{-1}(t)$ is an estimator matrix of $T_i^*(\rho_i)^{-1}$. The local estimation law is in conjunction with local internal model illustrated in Section 3.3.

As we did before, we convert the problem into a global stabilization problem in Section 5.1. To guarantee the stability of transformed system, we add one more coordinate transformation term inspired also by backstepping in the same section. An adaptive law is proposed in Section 5.2 and the stability of the system is formally analyzed in Section 5.3.

5.1 Coordinate transformation

Like Section 4.1, the coordinate transformation is to convert the global regulation problem into a global stabilization problem. Additional term is also inspired by backstepping and makes the system ISS with respect to neighboring states. Consider the coordinate transformation

$$\hat{x}_i(t) \triangleq x_i(t) - x_i^*(\Psi_i T_i^{-1}(t)\eta_i(t), t) - \hat{x}_i^*(t) \quad (18)$$

where $\hat{x}_i^*(t) = [0, \hat{x}_{i,2}^*(t), \hat{x}_{i,3}^*(t), 0, \hat{x}_{i,5}^*(t)]^T$ for $\forall i \in \mathcal{G}$, $\hat{x}_i^*(t) = [0, \hat{x}_{i,2}^*(t), -\hat{x}_{i,3}^*(t), \hat{x}_{i,5}^*(t)]^T$ for $\forall i \in \mathcal{L}$, $\hat{x}_i^*(t) = [0, 0]^T$ for $i \in \mathcal{T}$ and

$$\begin{aligned} \hat{x}_{i,2}^*(t) &\triangleq (1 - 2\pi)(x_{i,2}(t) - w^*) - k_{i,1}\hat{x}_{i,1}(t) \\ \hat{x}_{i,3}^*(t) &\triangleq \left(\frac{m_i}{2\pi}k_{i,1}^2 - \frac{D_i}{2\pi}k_{i,1} + \sum_{j \in \mathcal{N}_i} t_{ij}\right)\hat{x}_{i,1}(t) \\ &\quad + \left(\frac{D_i}{2\pi} - \frac{m_i}{2\pi}(k_{i,1} + k_{i,2})\right)\hat{x}_{i,2}(t) + \hat{x}_{i,4}(t) \\ &\triangleq e_{M_{i,1}}\hat{x}_{i,1}(t) + e_{M_{i,2}}\hat{x}_{i,2}(t) + \hat{x}_{i,4}(t) \\ \hat{x}_{i,5}^*(t) &\triangleq -\frac{m_i}{2\pi}N_i(\hat{x}_{i,2}(t) - k_{i,1}\hat{x}_{i,1}(t)). \end{aligned}$$

Under coordinate transformation (18), the frequency regulation problem is transformed to a stabilization problem for the same reason as (13). The difference is that we use estimator matrix $T_i^{-1}(t)$ instead of true matrix $T_i^*(\rho_i)^{-1}$. The origin of the system does not change

under the additional term $\hat{x}_i^*(t)$ in the coordinate transformation. Consider input

$$u_i(t) = u_i^*(\Psi_i T_i^{-1}(t) \eta_i(t), t) + \hat{u}_i^*(t) \quad (19)$$

where $\hat{u}_i^*(t) = [\hat{P}_{v_i}^*(t), \hat{\lambda}_i^*(t)]^T$ for $i \in \mathcal{G}$, $\hat{u}_i^*(t) = \hat{\lambda}_i^*(t) = -e_{M_{i,1}}(c_i + k_{i,1})\hat{x}_{i,1}(t) + (e_{M_{i,1}} - e_{M_{i,2}}(c_i + k_{i,2}))\hat{x}_{i,2}(t) + (c_i + k_{i,3} - \frac{e_{M_{i,2}}}{m_i})\hat{x}_{i,3}(t)$ for $i \in \mathcal{L}$, and

$$\begin{aligned} \hat{P}_{v_i}^*(t) &\triangleq e_{M_{i,1}}(1 - T_{CH_i} k_{i,1})\hat{\theta}_i(t) + (1 - T_{CH_i} k_{i,4})\hat{P}_{L_i}^E(t) \\ &\quad + (T_{CH_i} e_{M_{i,1}} + (1 - T_{CH_i} k_{i,2})e_{M_{i,2}})\hat{w}_i(t) \\ &\quad + (1 + \frac{2\pi}{m_i} T_{CH_i} e_{M_{i,2}} - T_{CH_i} k_{i,3})\hat{P}_{M_i}(t). \\ \hat{\lambda}_i^*(t) &\triangleq (c_i + k_{i,4})\hat{x}_{i,4}(t). \end{aligned}$$

Through coordinate transformation (18) and input (19), system (2) and (8), and internal model (12) become

$$\begin{aligned} \dot{\hat{x}}_{i,l}(t) &= -k_{i,l}\hat{x}_{i,l}(t) + B_{i,l,1}(T_i^*(\rho_i)^{-1})\hat{x}_i(t) \\ &\quad + B_{i,l,2}(\hat{T}_i^{-1}(t))x_i(t) + \sum_{j \in \mathcal{N}_i} B_{ij,l}\hat{x}_j(t) \\ \dot{\hat{x}}_{i,5}(t) &= M_i\hat{x}_{i,5}(t) + B_{i,5,1}\hat{x}_i(t) + \sum_{j \in \mathcal{N}_i} B_{ij,5}\hat{x}_j(t) \quad (20) \end{aligned}$$

where $B_{i,l,k}$, and $B_{ij,l}$ are corresponding constant matrices and $\hat{T}_i^{-1}(t) = T_i^{-1}(t) - T_i^*(\rho_i)^{-1}$. Analyzing the stability of dynamics (20) has potential difficulties because unknown constant matrix $T_i^*(\rho_i)^{-1}$ and $\hat{T}_i^{-1}(t)$ appear in $B_{i,2,1}$, $B_{i,3,1}$, $B_{i,2,2}$, and $B_{i,3,2}$.

5.2 Projected parameter estimator

In this section, we introduce parameter estimator dynamics of $T_i^{-1}(t)$. For notational simplicity, $t_{i,k}^* = [t_{i,k,1}^*, \dots, t_{i,k,2\ell}^*]$, $t_{i,k}(t) = [t_{i,k,1}(t), \dots, t_{i,k,2\ell}(t)]$, and $\hat{t}_{i,k}(t) = [\hat{t}_{i,k,1}(t), \dots, \hat{t}_{i,k,2\ell}(t)]$ denote the k^{th} row vector of $T_i^*(\rho_i)^{-1}$, $T_i^{-1}(t)$, and $\hat{T}_i^{-1}(t)$ respectively. Moreover, we define $\psi_{i,k}$ as the k^{th} element of $\Psi_i = [\psi_{i,1}, \dots, \psi_{i,2\ell}]$. We design parameter estimator $T_i^{-1}(t)$ as follows:

$$\begin{aligned} \dot{t}_{i,k}^T(t) &= \psi_{i,k}(J_i(t) - (\|J_i(t)\| + \gamma) \\ &\quad \times \text{sign}_{\frac{B(M_i)}{\|N_i\|}}(\psi_{i,k} t_{i,k}(t))) \quad (21) \end{aligned}$$

where $J_i(t) \triangleq \frac{2\pi}{m_i} x_{i,5}(t)(\hat{x}_{i,2}(t) - e_{M_{i,2}}\hat{x}_{i,3}(t))$ for $i \in \mathcal{G}$, $J_i(t) \triangleq \frac{2\pi}{m_i} x_{i,5}(t)(\hat{x}_{i,2}(t) + e_{M_{i,2}}\hat{x}_{i,3}(t))$ for $i \in \mathcal{L}$, $B(M_i) \triangleq (\rho_{\max}^2 + 1)\ell + \|M_i\|_F$, and $\gamma > 0$ is an arbitrary constant. The adaptive law $\dot{t}_{i,k}^T = \psi_{i,k} J_i(t)$ can also be implemented instead of (21). However, the extra term $(\|J_i(t)\| + \gamma) \text{sign}_{\frac{B(M_i)}{\|N_i\|}}(\psi_{i,k} t_{i,k}(t))$ in (21)

speeds up the convergence rate by restricting the parameter estimator's size within $\|\Psi_i T_i^{-1}(t)\| \leq \frac{2\ell B(M_i)}{\|N_i\|}$. To see this, assume we choose initial conditions $|t_{i,k,l}(t_0)| \leq \frac{B(M_i)}{\|N_i\| \|\psi_{i,k}\|}$ for $\forall i, k, l$. Moreover, suppose that $\psi_{i,k} t_{i,k,l}(t)$ is $\pm \frac{B(M_i)}{\|N_i\|}$ for some t , then its derivative is $\dot{t}_{i,k,l}^T(t) = \psi_{i,k}(j_{i,l}(t) \mp (\|J_i(t)\| + \gamma))$ where $J_i(t) \triangleq [j_{i,1}(t), \dots, j_{i,2\ell}(t)]^T$. Because $|j_{i,l}(t)| \leq \|J_i(t)\|$, state $t_{i,k,l}(t)$ remains $|\psi_{i,k} t_{i,k,l}(t)| \leq \frac{B(M_i)}{\|N_i\|}$ for $\forall t \geq t_0$. This implies $\|\psi_{i,k} t_{i,k}\| \leq \frac{\sqrt{2\ell} B(M_i)}{\|N_i\|}$ as well as $\|\Psi_i T_i^{-1}(t)\| \leq \frac{2\ell B(M_i)}{\|N_i\|}$ for $\forall t \geq t_0$.

5.3 Frequency regulation analysis

The following theorem summarizes the asymptotic stability of transformed system (20).

Algorithm 2 Control gain designs

- 1: Choose $\delta > 0$;
 - 2: **for** $i \in \mathcal{G}, \mathcal{L}$ **do**
 - 3: $k_{i,1} = \frac{3}{2} + \sqrt{2\ell} + \frac{\pi}{m_i} + \sum_{j \in \mathcal{N}_i} t_{ij}(\frac{2\pi}{m_j} + \sqrt{2\ell}) + \delta$;
 - 4: Choose a controllable pair $(M_i, \frac{C_i}{\|C_i\|})$;
 - 5: **end for**
 - 6: **for** $i \in \mathcal{G}, \mathcal{L}$ **do**
 - 7: $\alpha_i = \min\{1, \frac{4\pi}{(k_{i,1}+1)\|(m_i M_i + D_i I_{2\ell})\|}\}$;
 - 8: $N_i = \alpha_i \frac{C_i}{\|C_i\|}$;
 - 9: $k_{i,2} = \delta + \frac{1+\sqrt{2\ell}}{2} + \frac{\pi}{m_i} \sum_{j \in \mathcal{N}_i} t_{ij} + B(M_i) + \frac{k_{i,1}^2 B^2(M_i)}{2\sqrt{2\ell}} + \frac{\pi B^2(M_i)}{2m_i \alpha_i^2 \ell^2} + \frac{\alpha_i}{4\pi} \|(m_i M_i + D_i I_{2\ell})\|$;
 - 10: $k_{i,3} = e_{M_{i,2}}^2 \frac{\pi}{m_i} \sum_{j \in \mathcal{N}_i} t_{ij} + \frac{\pi}{m_i} + \frac{e_{M_{i,2}}^2 B^2(M_i)}{2\sqrt{2\ell}} + \frac{k_{i,1}^2 e_{M_{i,2}}^2 B^2(M_i)}{2\sqrt{2\ell}}$;
 - 11: (For $i \in \mathcal{G}$) $k_{i,4} > 0$;
 - 12: **end for**
-

Theorem 5.1 Under Assumptions 3.1, 3.2, 3.4, 3.5, and that (M_i, N_i) is controllable for $\forall i$, we apply distributed internal controllers (19) with adaptive internal model (12) and (21). Then, states with internal model $x_i(t)$, and inputs $u_i(t)$ described in (2), (8), and (12) for $i \in \mathcal{V}$ are asymptotically convergent to their manifolds (9) and $\vartheta_i(t)$ for any initial states $x_i(t_0)$, and $T_i^{-1}(t_0)$ if $\mathbf{A} + \mathbf{A}^T$ is Hurwitz where $\dot{\hat{\mathbf{x}}}(t) = \mathbf{A}\hat{\mathbf{x}}(t) + \mathbf{B}(\hat{\mathbf{T}}(t))\mathbf{x}(t)$ and $\mathbf{x}(t) = [x_{i_1}^T(t), x_{i_2}^T(t), \dots, x_{i_N}^T(t)]^T$, $\hat{\mathbf{x}}(t) = [\hat{x}_{i_1}^T(t), \hat{x}_{i_2}^T(t), \dots, \hat{x}_{i_N}^T(t)]^T$, $\hat{\mathbf{T}}(t) = [\hat{t}_{i_1,1}(t), \dots, \hat{t}_{i_1,2\ell}(t), \dots, \hat{t}_{i_N,1}(t), \dots, \hat{t}_{i_N,2\ell}(t)]^T$. Moreover, such control gains $k_{i,l}$ and matrices M_i and N_i always exist if $D_i > \sum_{j \in \mathcal{N}_i} t_{ij}$ for $\forall i \in \mathcal{T}$.

PROOF. We first prove that the networked system is stable if $\mathbf{A} + \mathbf{A}^T$ is Hurwitz. Assume $\mathbf{A} + \mathbf{A}^T$ is Hurwitz.

We choose Lyapunov candidate

$$\mathbf{V}(t) = \frac{1}{2} \begin{bmatrix} \hat{\mathbf{x}}^T(t) & \hat{\mathbf{T}}^T(t) \end{bmatrix} \begin{bmatrix} \hat{\mathbf{x}}(t) \\ \hat{\mathbf{T}}(t) \end{bmatrix}. \quad (22)$$

The Lie derivative of $\mathbf{V}(t)$ is

$$\begin{aligned} \dot{\mathbf{V}}(t) &= \frac{1}{2} \hat{\mathbf{x}}^T(t) (\mathbf{A} + \mathbf{A}^T) \hat{\mathbf{x}}(t) \\ &+ \sum_{i \in \mathcal{V}} \sum_{k=1}^{2\ell} \hat{t}_{i,k}(t) (\dot{\hat{t}}_{i,k}^T(t) + \psi_{i,k} J_i(t)) \end{aligned} \quad (23)$$

We formulate the proofs into several claim statements.

Claim A: $\|\Psi_i T_i^*(\rho_i)^{-1}\| \leq \frac{B(M_i)}{\|N_i\|}$.

PROOF. By taking post-multiply $T^*(\rho_i)^{-1}$ and taking Frobenius norm on both sides of Sylvester equation (11),

$$\begin{aligned} &\|N_i \Psi_i T_i^*(\rho_i)^{-1}\|_F \\ &\leq \|T_i^*(\rho_i) \Phi_i(\rho_i) T_i^*(\rho_i)^{-1}\|_F + \|M_i\|_F. \end{aligned} \quad (24)$$

By definition, $\|N_i \Psi_i T_i^*(\rho_i)^{-1}\|_F$ becomes

$$\|N_i \Psi_i T_i^*(\rho_i)^{-1}\|_F = \|N_i\|_F \|\Psi_i T_i^*(\rho_i)^{-1}\|_F. \quad (25)$$

Apply (25) and the norm relation $\|\cdot\|_F \leq \|\cdot\|_{tr}$ (Lemma 10 in [53]) to (24). Then we have

$$\begin{aligned} &\|N_i\|_F \|\Psi_i T_i^*(\rho_i)^{-1}\|_F \\ &\leq \|T_i^*(\rho_i) \Phi_i(\rho_i) T_i^*(\rho_i)^{-1}\|_{tr} + \|M_i\|_F \\ &= \|\Phi_i(\rho_i)\|_{tr} + \|M_i\|_F \leq (\rho_{\max}^2 + 1)\ell + \|M_i\|_F. \end{aligned}$$

Note that $\|\cdot\|_F = \|\cdot\|_2$ when its argument is a vector. ■

Claim A implies $|\psi_{i,k} t_{i,k,l}^*| \leq \frac{B(M_i)}{\|N_i\|}$ for $\forall i, k, l$.

Claim B: $\sum_{k=1}^{2\ell} \hat{t}_{i,k}(t) (\dot{\hat{t}}_{i,k}^T(t) + \psi_{i,k} J_i(t)) \leq 0$.

PROOF. Consider adaptive law (21). If $\psi_{i,k} = 0$, then $\dot{\hat{t}}_{i,k}(t) = 0$. Let $S_{i,k}^+(t)$ denote a set of indices l such that $\psi_{i,k} t_{i,k,l}(t) = \frac{B(M_i)}{\alpha_i}$. Likewise, $S_{i,k}^-(t) \triangleq \{l | \psi_{i,k} t_{i,k,l}(t) = -\frac{B(M_i)}{\alpha_i}\}$. Then,

$$\begin{aligned} &\sum_{k=1}^{2\ell} \hat{t}_{i,k}(t) (\dot{\hat{t}}_{i,k}^T(t) + \psi_{i,k} J_i(t)) \\ &= \sum_{k=1}^{2\ell} \psi_{i,k} \left(\sum_{l \in S_{i,k}^+(t)} (t_{i,k,l}^* - \frac{B(M_i)}{\alpha_i \psi_{i,k}}) (\|J_i(t)\| + \gamma) \right. \\ &\quad \left. - \sum_{l \in S_{i,k}^-(t)} (t_{i,k,l}^* + \frac{B(M_i)}{\alpha_i \psi_{i,k}}) (\|J_i(t)\| + \gamma) \right) \leq 0 \end{aligned}$$

where $|\psi_{i,k} t_{i,k,l}^*| \leq \frac{B(M_i)}{\|N_i\|}$ is applied. ■

Apply the properties of Claim B to (23) to get

$$\dot{\mathbf{V}}(t) \leq \hat{\mathbf{x}}^T(t) (\mathbf{A} + \mathbf{A}^T) \hat{\mathbf{x}}(t) \leq \lambda_{\max}(\mathbf{A} + \mathbf{A}^T) \|\hat{\mathbf{x}}(t)\|^2 \quad (26)$$

where $\mathbf{A} + \mathbf{A}^T$ is symmetric and $\lambda_{\max}(\mathbf{A} + \mathbf{A}^T) < 0$ by assumption. Multiply -1 and take integral from t_0 to ∞ on the both sides of (26) to have

$$\begin{aligned} -\lambda_{\max}(\mathbf{A} + \mathbf{A}^T) \int_{t_0}^{\infty} \|\hat{\mathbf{x}}(t)\|^2 dt &\leq -\int_{t_0}^{\infty} \dot{\mathbf{V}}_i(t) dt \\ &= \mathbf{V}_i(t_0) - \mathbf{V}_i(\infty) \end{aligned}$$

where $0 \leq \mathbf{V}_i(\infty) \leq \mathbf{V}_i(t_0) < \infty$ because $\dot{\mathbf{V}}(t)$ is non-increasing as shown in (26). Therefore by Barbalat's Lemma (Lemma 8.2 in [22]), and the uniform continuity of $\|\hat{\mathbf{x}}(t)\|^2$, value $\|\hat{\mathbf{x}}(t)\|^2$ asymptotically converges to zero.

This implies the asymptotic convergence of $\hat{x}_i(t)$ to zero, as well as the asymptotic convergence of $x_i(t)$, and $u_i(t)$ to their manifolds. The uniform continuity of $\|\hat{\mathbf{x}}(t)\|^2$ is proven in Claim C.

Claim C: $\|\hat{\mathbf{x}}(t)\|^2$ is a uniformly continuous function.

PROOF. The value $\|\hat{\mathbf{x}}(t)\|$ is uniformly bounded by some constant U because $\|\hat{\mathbf{x}}(t)\|^2 \leq 2\mathbf{V}(t_0)$. Consider

$$\begin{aligned} &|\|\hat{\mathbf{x}}(t+\tau)\|^2 - \|\hat{\mathbf{x}}(t)\|^2| \\ &= \sum_{i \in \mathcal{V}} \left| \sum_{l=1}^5 (\|\hat{x}_{i,l}(t+\tau)\|^2 - \|\hat{x}_{i,l}(t)\|^2) \right| \\ &\leq \sum_{i \in \mathcal{V}} \left| \sum_{l=1}^5 \|\hat{x}_{i,l}(t+\tau)\|^2 - \|\hat{x}_{i,l}(t)\|^2 \right|. \end{aligned} \quad (27)$$

The term $\hat{x}_{i,l}(t+\tau)$ is given by $\hat{x}_{i,l}(t+\tau) = \hat{x}_{i,l}(t) + \int_t^{t+\tau} \dot{\hat{x}}_{i,l}(t) dt$. By uniform boundedness of all $\hat{x}_{i,l}(t)$, for $\forall l \in \{1, 2, 3, 4, 5\}$ and any $\tau > 0$,

$$\hat{x}_{i,l}(t) - a_{i,l}\tau \leq \hat{x}_{i,l}(t+\tau) \leq \hat{x}_{i,l}(t) + a_{i,l}\tau$$

where $a_{i,1}, a_{i,2}, a_{i,3}$, and $a_{i,4}$ are positive constants and $a_{i,5} = a[1, \dots, 1]^T$ is a vector with a positive constant a . Therefore,

$$\begin{aligned} |\|\hat{x}_{i,l}(t+\tau)\|^2 - \|\hat{x}_{i,l}(t)\|^2| &\leq \|2a_{i,l}^T \hat{x}_{i,l}(t) \tau\| + \|2a_{i,l}^T a_{i,l} \tau^2\| \\ &\leq \|2a_{i,l} U \tau\| + \|2a_{i,l}^T a_{i,l} \tau^2\| \end{aligned}$$

where this is a strictly increasing function of τ and $|\|\hat{x}_{i,l}(t+\tau)\|^2 - \|\hat{x}_{i,l}(t)\|^2| \rightarrow 0$ as $\tau \rightarrow 0$. By applying these relations to (27), we can prove the uniform continuity of $\|\mathbf{x}(t)\|^2$; i.e., for any given $\epsilon > 0$, there

always exists $\delta > 0$ such that for all $0 \leq \tau \leq \delta$, $|\|\mathbf{x}(t+\tau)\|^2 - \|\mathbf{x}(t)\|^2| \leq \epsilon$. ■

Claim C completes the proof for the stability part.

Now we proceed to prove that there always exists a set of control gains and matrices such that $\mathbf{A} + \mathbf{A}^T$ is negative definite by construction. Especially, Algorithm 2 generates such set. To prove this, assume we choose a set of control gains and matrices through Algorithm 2. It is not difficult to show that the chosen control gains and matrices satisfy

$$\begin{aligned} k_{i,1} &> p_{i,1} + \sum_{j \in \mathcal{N}_i} t_{ij} \left(\frac{\pi}{m_j} (1 + \beta_{j,3} e_{M_{i,2}}) + \frac{\sqrt{2\ell}\alpha_j}{2} \right), \\ k_{i,2} &> p_{i,2}, \quad k_{i,3} > p_{i,3}, \quad k_{i,4} > p_{i,4}, \quad -\lambda_{\max}(M_i) > p_{i,5} \end{aligned} \quad (28)$$

where

$$\begin{aligned} p_{i,1} &\triangleq \frac{1}{2} + \frac{\pi}{m_i} + \frac{k_{i,1}B(M_i)}{2\beta_{i,1}} + \frac{k_{i,1}e_{M_{i,2}}B(M_i)}{2\beta_{i,5}} \\ &\quad + \frac{\alpha_i k_{i,1}}{4\pi} \|(m_i M_i + D_i I_{2\ell})C\| + \frac{\sqrt{2\ell}\alpha_i}{2} \sum_{j \in \mathcal{N}_i} t_{ij} \\ p_{i,2} &\triangleq \frac{1}{2} + \frac{B(M_i)}{2} (\beta_{i,1} k_{i,1} + \frac{e_{M_{i,2}}}{\beta_{i,4}}) + \frac{\pi}{m_i} \sum_{j \in \mathcal{N}_i} t_{ij} \\ &\quad + \frac{\pi B(M_i)}{\sqrt{2\ell} m_i \alpha_i \beta_{i,2}} + \frac{\alpha_i}{4\pi} \|(m_i M_i + D_i I_{2\ell})C\| + B(M_i) \\ p_{i,3} &\triangleq e_{M_{i,2}} \frac{\pi}{m_i \beta_{i,3}} \sum_{j \in \mathcal{N}_i} t_{ij} + \frac{\pi}{m_i} + \frac{e_{M_{i,2}} B(M_i) \beta_{i,4}}{2} \\ &\quad + \frac{k_{i,1} e_{M_{i,2}} B(M_i) \beta_{i,5}}{2} \\ p_{i,5} &\triangleq \frac{\pi B(M_i) \beta_{i,2}}{\sqrt{2\ell} m_i \alpha_i} + \frac{\alpha_i (1 + k_{i,1})}{4\pi} \|(m_i M_i + D_i I_{2\ell})C\| \\ &\quad + \sqrt{2\ell} \alpha_i \sum_{j \in \mathcal{N}_i} t_{ij} \end{aligned}$$

$$\text{with } p_{i,4} \triangleq 0, \quad \beta_{i,1} = \frac{k_{i,1} B(M_i)}{\sqrt{2\ell}}, \quad \beta_{i,2} = \frac{\sqrt{2\ell} \alpha_i}{B(M_i)}, \quad \beta_{i,3} = \frac{1}{e_{M_{i,2}}}, \quad \beta_{i,4} = \frac{e_{M_{i,2}} B(M_i)}{\sqrt{2\ell}}, \quad \text{and } \beta_{i,5} = \frac{k_{i,1} e_{M_{i,2}} B(M_i)}{\sqrt{2\ell}}.$$

Now, again consider Lyapunov candidate (22) and its Lie derivative (23) for $i \in \mathcal{G}, \mathcal{L}$. In Theorem 4.1, it has been proven that system for $i \in \mathcal{T}$ is ISS contraction mappings with respect to neighboring states. Thus, there exists ISS Lyapunov function for $i \in \mathcal{T}$ (Theorem 1 in [52]). We apply some properties to equation (23). The first one is $\|N_i\| \leq \alpha_i \| [1, \dots, 1]^T \| = \alpha_i \sqrt{2\ell}$. The second one is $\|\Psi_i T_i^*(\rho_i)^{-1}\| \leq \frac{B_i(M_i)}{\sqrt{2\ell} \alpha_i}$ coming from Claim A. The last one is $2xy \leq \beta x^2 + y^2/\beta$ for any positive constant β . By applying these properties to (23), it becomes, for any

positive constants $\beta_{i,1}, \beta_{i,2}, \beta_{i,3}, \beta_{i,4}$, and $\beta_{i,5}$,

$$\begin{aligned} \dot{\mathbf{V}}(t) &\leq \sum_{i \in \mathcal{T}} \dot{V}_i(t) + \sum_{i \in \mathcal{G}, \mathcal{L}} \left(\sum_{l=1}^5 (-k_{i,l} + p_{i,l}) \|\hat{x}_{i,l}(t)\|^2 \right. \\ &\quad \left. + \sum_{j \in \mathcal{N}_i} t_{ij} \left(\frac{\pi}{m_i} (1 + \beta_{i,3} e_{M_{i,2}}) + \frac{\sqrt{2\ell}\alpha_i}{2} \right) \|\hat{x}_{j,1}(t)\|^2 \right) \\ &= \sum_{i \in \mathcal{V}} \left(-k_{i,1} + p_{i,1} + \sum_{j \in \mathcal{N}_i} t_{ij} \left(\frac{\pi}{m_i} (1 + \beta_{i,3} e_{M_{i,2}}) \right. \right. \\ &\quad \left. \left. + \frac{\sqrt{2\ell}\alpha_i}{2} \right) \|\hat{x}_{i,1}(t)\|^2 + \sum_{l=2}^5 (-k_{i,l} + p_{i,l}) \|\hat{x}_{i,l}(t)\|^2 \right) \end{aligned} \quad (29)$$

where $k_{i,5} = \lambda_{\max}(M_i)$ and $\dot{V}_i(t)$ is negative definite. By plugging (28) into (29), we have

$$\dot{\mathbf{x}}^T(t) (\mathbf{A} + \mathbf{A}^T) \dot{\mathbf{x}}(t) = \dot{\mathbf{V}}(t) \leq \dot{\mathbf{x}}^T(t) \bar{\mathbf{A}} \dot{\mathbf{x}}(t)$$

where matrix $\bar{\mathbf{A}}$ is Negative definite. Therefore, matrix $\mathbf{A} + \mathbf{A}^T$ is also Hurwitz. ■

Theorem 5.1 states a sufficient condition of system stability. The Lie derivative of Lyapunov candidate can only be negative semidefinite because the parameter adaptive error terms are sign indefinite. The existence of stabilizing control gains and matrices is guaranteed by Algorithm 2. Again, the algorithm shows another extreme; it is always possible to choose a set of stabilizing gains and matrices even when only local information are available, but is might be conservative. It is obvious that Algorithm 2 can be followed only with local system information.

Applying the approach used in this section to the fourth order system has potential difficulties. Manifold $P_{M_i}^*(t)$ depends on $T_i^{-1}(t)$ because we want $P_{M_i}(t)$ to cancels $P_{ren_i}^L = \Psi_{i,1} T_i^*(\rho_i)^{-1} \vartheta_i$. This term affects manifold $P_{v_i}^*(t)$ which should be a function of $\tilde{T}_i^{-1}(t)$. Likewise, $P_{ref_i}^*$ will be a function of $\tilde{T}_i^{-1}(t)$ which depends on unmeasurable terms $T_i^*(\rho_i)^{-1}$ and $\vartheta_i(t)$.

6 Simulation

In this section, we present simulations to show the performance of the proposed controllers. Most of parameters are adopted from [3,26]. We, however, choose relatively high frequencies of wind generations to inspect evolutions of $P_{M_i}(t)$ and $P_{L_i}^E(t)$ in a short time. By Van der Hoven's spectrum model [56], proper frequencies are around $\rho_i^L \approx 5.0 \times 10^{-5} rad$ and $\rho_i^M \approx 5.0 \times 10^{-4} rad$ but higher frequencies $\rho_i^L = 0.1 rad$, and $\rho_i^M = 0.2 rad$ are chosen instead in this simulation.

The controllers are applied to the single line diagram of the IEEE 68-bus test system topology shown in [38,44]. The topology includes 16 generators ($|\mathcal{G}| = 16$), 24 load buses ($|\mathcal{L}| = 24$) and 28 load bus with zero load ($|\mathcal{T}| = 28$). We assume that each generator/load bus $i \in \mathcal{G}, \mathcal{L}$ has a local wind turbine. For $\forall i \in \mathcal{G}$, each wind turbine generates $P_{ren_i}(t) = 300 \sin(0.1t)$, and, for $\forall i \in \mathcal{L}$, each wind turbine generates $P_{ren_i}(t) = 300 \sin(0.1t) + 400 \sin(0.2t)$. On the test system topology, we simulate both the *robust (adaptive) frequency regulation* problems proposed in Section 4 and 5. Moreover, we conduct one more simulation to compare the effect of connection and disconnection of wind power generations with other controllers.

6.1 Parameters and Matrices

The parameters are adopted from page 598 in [26]: $m_i = 10s$, $R_i = 0.05Hz/MW$, $T_{CH_i} = 0.3s$, $T_{G_i} = 0.2s$, and $t_{ij} = 1.5MW/rad$ for $\forall i \in \mathcal{V}$. Load damping constants are $D_i = 1MW/Hz$ for $i \in \mathcal{G}, \mathcal{L}$ and $D_i = 15MW/Hz$ for $i \in \mathcal{T}$, and the manifolds as $w_i^* = 60Hz$. Demand response parameters $b'_i = 40\$/MWh$ and $c'_i = -0.8\$/MW^2h$ and $\tau_i = 150s$ are borrowed from [3]. We set the manifolds as $w_i^* = 60Hz$ and inelastic demands are $P_{L_i}^{IE}(t) = 100 + 50 \sin(0.01t)$ for $\forall i \in \mathcal{L}$.

Wind power generators with $P_{ren_i}(t) = 300 \sin(t)$ and $\Psi_i = [10, 0]$ are attached to generator buses $i \in \mathcal{G}$. Load buses $i \in \mathcal{L}$ have wind power generators with $P_{ren_i}^L(t) = 300 \sin(t)$, $P_{ren_i}^M(t) = 400 \sin(2t)$, $\Psi_{i,1} = [10, 0, 0, 0]$ and $\Psi_{i,2} = [0, 0, 10, 0]$. Note that one can choose maximum frequency of wind power generation signals by choosing a proper time constant T in the BESS.

For the *robust frequency regulation* problem, we choose the following set of control gains and matrices for $i \in \mathcal{G}$ and $i \in \mathcal{L}$, respectively: $k_i = [5, 10, 15, 35, 3]^T$, $k_i = [5, 10, 15]^T$ and matrices

$$M_i = \begin{bmatrix} -2 & 0 \\ 11 & -2.5 \end{bmatrix}, M_i = \begin{bmatrix} -2 & 0 & 0 & 0 \\ 11 & -2.5 & 0 & 0 \\ 4 & -1 & -3 & 0 \\ -6 & 5 & 1 & -3.5 \end{bmatrix} \quad (30)$$

with $N_i = [1, 1]^T$, $N_i = [1, 1, 1, 1, 1]^T$. Such sets of the gains and matrices satisfy that matrix \mathbf{A} is Hurwitz.

For the *robust adaptive frequency regulation* problem, we choose the following set of control gains and matrices for $i \in \mathcal{G}$ and $i \in \mathcal{L}$, respectively: $k_i = [15, 20, 40, 3]^T$, $k_i = [15, 20, 40]^T$ and matrices (30) with $N_i = [1, 1]^T$, $N_i = [1, 1, 1, 1]^T$. Such sets of the gains and matrices satisfy that matrix $\mathbf{A} + \mathbf{A}^T$ is Hurwitz.

6.2 Simulation Results

To regulate angular frequency to $60Hz$, we aim that each demand response $P_{L_i}^E(t)$ in $i \in \mathcal{L}$ tracks low and medium frequency parts of local wind power generations, and mechanical generation $P_{M_i}(t)$ in $i \in \mathcal{G}$ tracks low frequency parts of local wind power generations.

6.2.1 Robust frequency regulation

The results are shown in Figures 3. In each subfigures, the horizontal axis represents time and the vertical axis represents corresponding values. The first subfigure shows that angular frequency of bus $1 \in \mathcal{L}$ converges to $60Hz$ exponentially. All the states also converge to their manifolds as shown in the second subfigure; i.e., the designed distributed controllers achieve the objective and eventually regulate network-wide frequencies to $60Hz$. Mechanical power and elastic demand are used to balance the power generation and usage by tracking wind power generations. Especially, the trajectory of elastic demand $P_{L_1}^E(t)$ of bus $1 \in \mathcal{L}$ tracks desired signals, low and medium frequency parts of wind power generations and stabilizing signals; i.e., $P_{L_i}^{E*}(t) = -P_{L_i}^{IE}(t) + P_{ren_i}(t) - D_i w^* - \sum_{j \in \mathcal{N}_i} P_{ij}^*$ as shown in the third subfigure. The last subfigure presents the trajectory of mechanical generation $P_{M_{68}}(t)$ of bus $68 \in \mathcal{G}$ tracks low frequency parts of wind power generations and stabilizing signals; i.e., $P_{M_i}^*(t) = P_{L_i}^{IE}(t) - P_{ren_i}^L(t) + D_i w^* + \sum_{j \in \mathcal{N}_i} P_{ij}^*$. We intentionally choose very low frequency $0.01rad$ of inelastic demand signal $P_{L_i}^{IE}(t)$ to see whether $P_{L_i}^E(t)$ and $P_{M_i}(t)$ follows sinusoidal wind power generations $P_{ren_i}(t)^L$ and $P_{ren_i}(t)$, respectively.

6.2.2 Robust adaptive frequency regulation

As shown in the figure 4, angular frequency is regulated to $60Hz$. The second subfigure shows that network-wide state errors with respect to their manifolds converge to zero; i.e., the controllers achieve frequency regulation. The angular frequency regulation is achieved by the fact that each $P_{L_1}^E(t)$ and $P_{M_{68}}(t)$ follow the desired manifolds, balancing power where $1 \in \mathcal{L}$ and $68 \in \mathcal{G}$; low and medium frequency parts and low frequency parts.

6.2.3 Robust frequency regulation - Comparison

We conduct one more simulation of *Robust frequency regulation* problem. However at this time, wind power generations are connected at time $10s$ and disconnected at time $120s$. Furthermore, the frequency fluctuation of the proposed controllers is compared with regular distributed controllers without internal model. For a fair comparison, synchronous generators in generator buses and demand response in load buses are both used to stabilize the frequencies in the both simulations.

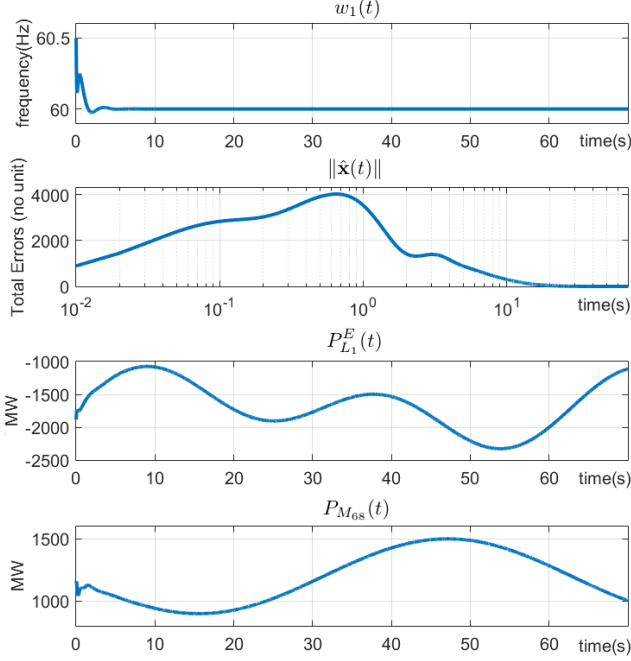


Fig. 3. (*robust frequency regulation*) Frequency fluctuation $w_1(t)$ of bus $1 \in \mathcal{L}$, network-wide state errors to their manifolds $\|\tilde{x}(t)\|$, elastic demand $P_{L_1}^E(t)$ trajectory and mechanical generation $P_{M_{68}}(t)$ trajectory.

Regular distributed controllers suppress the frequency fluctuation and its amplitude will decrease as its control gains increase, but cannot completely reject the fluctuation. Unlike the regular controllers, when wind power generators are connected to the system, the proposed distributed controllers with internal model are able to completely reject the disturbances induced by wind power generations. With the disconnection of wind power generator, the frequencies also converge to desired point $60Hz$ exponentially because the system without wind power generators is a special case of the system which we are dealing with in the paper.

7 Conclusions

We have proposed distributed controllers for *robust (adaptive) frequency regulation* problems under fast changing and unknown wind generations. We adopt local internal model (and adaptive technique) to cope with uncertainties. To overcome fast changing natures of uncertain signals, two of new grid components are integrated. At each bus with wind power generations, a BESS filters out high frequency parts of unknown signals. At generator bus, demand response tracks its medium frequency parts and synchronous generator tracks low frequency parts and stabilizes the system. At load bus, demand response tracks both low and medium frequency components and stabilize the local system.

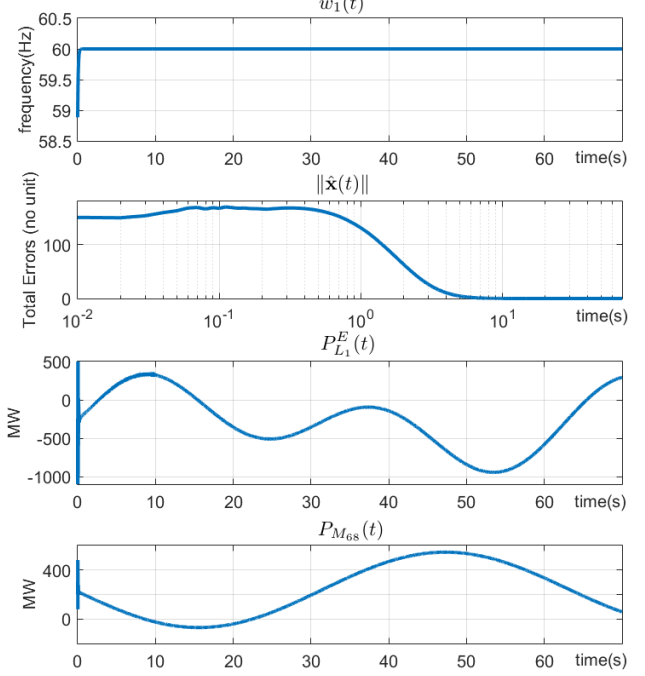


Fig. 4. (*robust adaptive frequency regulation*) Frequency fluctuation $w_1(t)$ of bus $1 \in \mathcal{L}$, network-wide state errors to their manifolds $\|\tilde{x}(t)\|$, elastic demand $P_{L_1}^E(t)$ trajectory and mechanical generation $P_{M_{68}}(t)$ trajectory.

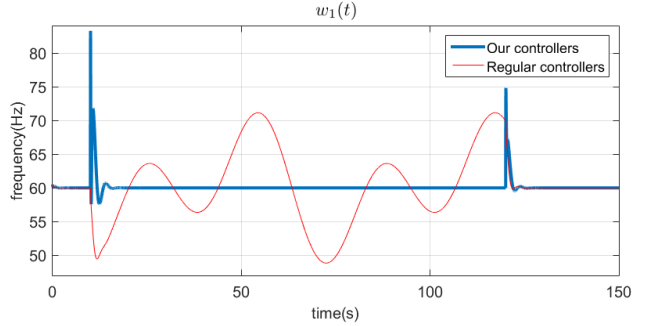


Fig. 5. (*robust frequency regulation*) Frequency $w_1(t)$ fluctuations of bus 1 under the proposed distributed controllers (bold) and regular stabilizing distributed controllers (thin). Wind power generators are suddenly connected at 10s and disconnected at 120s.

APPENDIX

Distributed constrained small gain theorem is introduced in this appendix. The theorem is an extension of constrained small-gain theorem in [63] to a network set-up.

Consider an undirected graph $(\mathcal{V}, \mathcal{E})$ and set $\mathcal{N}_i \triangleq \{j \in \mathcal{V} \setminus \{i\} | (i, j) \in \mathcal{E}\}$. The dynamic system associated with node i is given by

$$\dot{x}_i(t) = f_i(x(t), d_i(t), t) \quad (31)$$

where $x_i(t)$ and $d_i(t)$ denote system state and uncertainty respectively.

Assumption 7.1 *The system (31) is input-to-state stable with respect to neighboring states. Equivalently, there exist a class \mathcal{KL} function β_i and class \mathcal{K} functions γ_{id} and γ_{ij} such that for $\forall t \geq t_0$ and $\forall i \in \mathcal{V}$,*

$$\|x_i(t)\| \leq \max\{\beta_i(\|x_i(t_0)\|, t - t_0), \gamma_{id}(\|d(t)\|_{[t_0, t]}), \max_{j \in \mathcal{N}_i} \{\gamma_{ij}(\|x_j\|_{[t_0, t]})\}\}. \quad (32)$$

Assumption 7.2 *Gain functions γ_{ij} are contraction mappings for $(i, j) \in \mathcal{E}$; i.e., $\gamma_{ij}(s) < s$ for all $s > 0$.*

Theorem 7.1 (Distributed constrained small gain theorem) *Under Assumptions 7.1 and 7.2, the system (31) is ISS with respect to d . Equivalently, there exists class \mathcal{KL} function β and class \mathcal{K} function γ_{id} such that for all $x_i(t_0) \in \hat{X}_i$ and $\|d\|_{[t_0, \infty)} < \hat{\Delta}_d$, the solution of (31) exists and for $\forall t \geq t_0$,*

$$\|x(t)\| \leq \max\{\beta(\|x(t_0)\|, t - t_0), \gamma_{id}(\|d(t)\|_{[t_0, t]})\}. \quad (33)$$

Moreover, the function $\beta(x, t) = |\mathcal{V}| \sum_{i \in \mathcal{V}} \beta_i(|\mathcal{V}| \sum_{k \in \mathcal{V}} \beta_k(x, 0), \frac{t}{(2\mathcal{L})^{|\mathcal{V}|-1}})$ is a class \mathcal{KL} function candidate of $\beta(\cdot)$ in (33) where $\mathcal{L} > 1$ is a constant.

PROOF. For the notational simplicity in the sequent proof, we assume that \mathcal{V} is complete; i.e., $\mathcal{N}_i = \mathcal{V} \setminus \{i\}$. If $(i, j) \notin \mathcal{E}$, then $\gamma_{ij}(s) = s$. We divide the remaining of the proof into three claims.

Claim 1: We will prove by induction that the following hold for $i \in S_\ell \triangleq \{1, \dots, \ell\}$:

$$\begin{aligned} \|x_i\|_{[t_0, T]} &\leq \max\{\beta_i(\|x_i(t_0)\|, 0), \\ &\max_{(i, i_1, \dots, i_\kappa) \in \mathcal{P}_{ii_\kappa}} \gamma_{ii_1} \circ \dots \circ \gamma_{i_{\kappa-1}i_\kappa} \circ \gamma_{i_\kappa d}(\|d_{i_\kappa}\|_{[t_0, T]}), \\ &\max_{i_1, \dots, i_\kappa \in S_\ell} \max_{j \in S_\ell \setminus \{i\}} \max_{(j, i_\kappa, \dots, i) \in \mathcal{P}_{ji}} \gamma_{ii_1} \circ \dots \circ \gamma_{i_{\kappa-1}i_\kappa} \circ \gamma_{i_\kappa j}(\|x_j\|_{[t_0, T]})\}, \\ &\gamma_{ii_1} \circ \gamma_{i_1 i_2} \circ \dots \circ \gamma_{i_{\kappa-1}i_\kappa} \circ \beta_j(\|x_j(t_0)\|, 0), \\ &\max_{j \notin S_\ell} \max_{(i, i_1, \dots, i_\kappa, j) \in \mathcal{P}_{ij}} \gamma_{ii_1} \circ \dots \circ \gamma_{i_{\kappa-1}i_\kappa} \circ \gamma_{i_\kappa j}(\|x_j\|_{[t_0, T]})\}. \end{aligned} \quad (34)$$

PROOF. By (32), one can see that

$$\|x_1\|_{[t_0, T]} \leq \max\{\beta_1(\|x_1(t_0)\|, 0), \gamma_{1d}(\|d_1\|_{[t_0, T]}), \max_{j \neq 1} \{\gamma_{1j}(\|x_j\|_{[t_0, T]})\}\}, \quad (35)$$

and

$$\|x_2\|_{[t_0, T]} \leq \max\{\beta_2(\|x_2(t_0)\|, 0), \gamma_{2d}(\|d_2\|_{[t_0, T]}), \max_{j \neq 2} \{\gamma_{2j}(\|x_j\|_{[t_0, T]})\}\}. \quad (36)$$

Substitute (36) into (35), and it renders the following:

$$\begin{aligned} \|x_1\|_{[t_0, T]} &\leq \max\{\beta_1(\|x_1(t_0)\|, 0), \gamma_{1d}(\|d_1\|_{[t_0, T]}), \\ &\gamma_{12} \circ \beta_2(\|x_2(t_0)\|, 0), \gamma_{12} \circ \gamma_{2d}(\|d_2\|_{[t_0, T]}), \\ &\max_{j \neq 2} \{\gamma_{12} \circ \gamma_{2j}(\|x_j\|_{[t_0, T]})\}, \\ &\max_{j \notin \{1, 2\}} \{\gamma_{1j}(\|x_j\|_{[t_0, T]})\}\}. \end{aligned} \quad (37)$$

Since $\gamma_{12} \circ \gamma_{21}$ is a contraction mapping, it follows from (37) that

$$\begin{aligned} \|x_1\|_{[t_0, T]} &\leq \max\{\beta_1(\|x_1(t_0)\|, 0), \gamma_{1d}(\|d_1\|_{[t_0, T]}), \\ &\gamma_{12} \circ \beta_2(\|x_2(t_0)\|, 0), \gamma_{12} \circ \gamma_{2d}(\|d_2\|_{[t_0, T]}), \\ &\max_{j \notin \{1, 2\}} \{\max\{\gamma_{1j}, \gamma_{12} \circ \gamma_{2j}\}(\|x_j\|_{[t_0, T]})\}\}. \end{aligned} \quad (38)$$

By symmetry, one can show a similar property to (38) for $\|x_2\|_{[t_0, T]}$. So (34) holds for the case of $\ell = 2$. Now assume that (34) holds for some $\ell < n$. Similar to (35), we have

$$\begin{aligned} \|x_{\ell+1}\|_{[t_0, T]} &\leq \max\{\beta_{\ell+1}(\|x_{\ell+1}(t_0)\|, 0), \\ &\gamma_{(\ell+1)d}(\|d_{\ell+1}\|_{[t_0, T]}), \max_{j \neq (\ell+1)} \{\gamma_{(\ell+1)j}(\|x_j\|_{[t_0, T]})\}\}. \end{aligned} \quad (39)$$

Following analogous steps above, one can show that (35) holds for $\ell + 1$. By induction, we complete the proof. ■

Claim 2: We show by contradiction the existence and boundedness of the solution to (31).

PROOF. A direct result of Claim 1 is that the following holds for all $i \in \mathcal{V}$:

$$\begin{aligned} \|x_i\|_{[t_0, T]} &\leq \max\{\beta_i(\|x_i(t_0)\|, 0), \\ &\max_{(i, i_1, \dots, i_\kappa) \in \mathcal{P}_{ii_\kappa}} \gamma_{ii_1} \circ \dots \circ \gamma_{i_{\kappa-1}i_\kappa} \circ \gamma_{i_\kappa d}(\|d_{i_\kappa}\|_{[t_0, T]}), \\ &\max_{j \neq i} \max_{(j, i_\kappa, \dots, i) \in \mathcal{P}_{ji}} \gamma_{ii_1} \circ \dots \circ \gamma_{i_{\kappa-1}i_\kappa} \circ \gamma_{i_\kappa j} \circ \beta_j(\|x_j(t_0)\|, 0)\}. \end{aligned} \quad (40)$$

Since all the gain functions γ_{ij} are contraction mappings, (40) renders the following:

$$\begin{aligned} \|x_i\|_{[t_0, T]} &\leq \max\{\beta_i(\|x_i(t_0)\|, 0), \\ &\max_{j \in \mathcal{N}_i} \gamma_{ij} \circ \gamma_{jd}(\|d_j\|_{[t_0, T]}), \max_{j \in \mathcal{N}_i} \beta_j(\|x_j(t_0)\|, 0)\}. \end{aligned} \quad (41)$$

Because of the choice of $x_i(t_0)$ and the bound on d , the relation (40) holds for any T . It implies that

$$\|x_i(t)\| \leq \max\{\beta_i(\|x_i(t_0)\|, 0), \hat{\Delta}_d, \max_{j \in \mathcal{N}_i} \beta_j(\|x_j(t_0)\|, 0)\}.$$

for all $t \geq t_0$ and thus is uniformly bounded. It completes the proof. ■

Claim 3: We show the ISS property of (31). We will prove by induction that the following holds for all $i \in S_\ell \triangleq \{1, \dots, \ell\}$:

$$\|x_i(t)\| \leq \max\{\tilde{\beta}_i^{[\ell-1]}(\|x\|_\infty, t - t_0), \gamma_i^{[\ell-1]}(\|d\|_{[t_0, t]}), \max_{j \notin S_\ell} \max_{(i, i_1, \dots, i_\kappa, j) \in \mathcal{P}_{ij}} \gamma_{ii_1} \circ \dots \circ \gamma_{i_\kappa j}(\|x_j\|_{[t_0, t]})\}, \quad (42)$$

for some class \mathcal{KL} function $\tilde{\beta}_i^{[\ell-1]}$ where $\|x\|_\infty \triangleq \sup\{\|x(t)\| \mid t \in [t_0, \infty)\}$.

PROOF. Let $\ell = 2$. Note that for any constant $\mathcal{L} > 1$,

$$\begin{aligned} \|x_1(t_0 + T)\| &\leq \max\{\beta_1(\|x_1(t_0 + \frac{2\mathcal{L}-1}{2\mathcal{L}}T)\|, \frac{1}{2\mathcal{L}}T), \\ \gamma_{1d}(\|d_1\|_{[t_0 + \frac{2\mathcal{L}-1}{2\mathcal{L}}T, t_0 + T]}), \max_{j \neq 1} \gamma_{1j}(\|x_j\|_{[t_0 + \frac{2\mathcal{L}-1}{2\mathcal{L}}T, t_0 + T]})\} \\ &\leq \max\{\beta_1(\|x\|_\infty, \frac{1}{2\mathcal{L}}T), \gamma_{1d}(\|d_1\|_{[t_0 + \frac{2\mathcal{L}-1}{2\mathcal{L}}T, t_0 + T]}), \\ \max_{j \neq 1} \gamma_{1j}(\|x_j\|_{[t_0 + \frac{2\mathcal{L}-1}{2\mathcal{L}}T, t_0 + T]})\}. \end{aligned} \quad (43)$$

For any $\tau_2 \in [\frac{2\mathcal{L}-1}{2\mathcal{L}}T, T]$, it holds that

$$\begin{aligned} \|x_2(t_0 + \tau_2)\| &\leq \max\{\beta_2(\|x_2(t_0 + \frac{2\mathcal{L}-2}{2\mathcal{L}}T)\|, \tau_2 - \frac{2\mathcal{L}-2}{2\mathcal{L}}T), \\ \gamma_{2d}(\|d_2\|_{[t_0 + \frac{2\mathcal{L}-2}{2\mathcal{L}}T, t_0 + \tau_2]}), \\ \max_{j \neq 2} \gamma_{2j}(\|x_j\|_{[t_0 + \frac{2\mathcal{L}-2}{2\mathcal{L}}T, t_0 + \tau_2]})\} \\ &\leq \max\{\beta_2(\|x\|_\infty, \frac{1}{\mathcal{L}}T), \gamma_{2d}(\|d_2\|_{[t_0 + \frac{2\mathcal{L}-2}{2\mathcal{L}}T, t_0 + T]}), \\ \max_{j \neq 2} \gamma_{2j}(\|x_j\|_{[t_0 + \frac{2\mathcal{L}-2}{2\mathcal{L}}T, t_0 + T]})\}. \end{aligned} \quad (44)$$

So (44) implies that

$$\begin{aligned} \|x_2\|_{[t_0 + \frac{2\mathcal{L}-1}{2\mathcal{L}}T, t_0 + T]} &\leq \max\{\beta_2(\|x\|_\infty, \frac{1}{\mathcal{L}}T), \\ \gamma_{2d}(\|d_2\|_{[t_0 + \frac{2\mathcal{L}-2}{2\mathcal{L}}T, t_0 + T]}), \\ \max_{j \neq 2} \gamma_{2j}(\|x_j\|_{[t_0 + \frac{2\mathcal{L}-2}{2\mathcal{L}}T, t_0 + T]})\}. \end{aligned} \quad (45)$$

Substitute (45) into (43), and we have

$$\begin{aligned} \|x_1(t_0 + T)\| &\leq \max\{\beta_1(\|x\|_\infty, \frac{1}{2\mathcal{L}}T), \gamma_{1d}(\|d_1\|_{[t_0 + \frac{2\mathcal{L}-2}{2\mathcal{L}}T, t_0 + T]}), \\ \gamma_{12} \circ \beta_2(\|x\|_\infty, \frac{1}{\mathcal{L}}T), \gamma_{12} \circ \gamma_{2d}(\|d_2\|_{[t_0 + \frac{2\mathcal{L}-2}{2\mathcal{L}}T, t_0 + T]}), \\ \gamma_{12} \circ \gamma_{21}(\|x_1\|_{[t_0 + \frac{2\mathcal{L}-2}{2\mathcal{L}}T, t_0 + T]}), \\ \max_{j \notin S_2} \max\{\gamma_{1j}, \gamma_{12} \circ \gamma_{2j}\}(\|x_j\|_{[t_0 + \frac{2\mathcal{L}-2}{2\mathcal{L}}T, t_0 + T]})\}. \end{aligned} \quad (46)$$

Since $\gamma_{12} \circ \gamma_{21}(\cdot)$ is a contraction mapping, there is class \mathcal{KL} function $\tilde{\beta}_1$ such that

$$\begin{aligned} \|x_1(t)\| &\leq \max\{\tilde{\beta}_1(\|x\|_\infty, t - t_0), \\ \gamma_{1d}(\|d_1\|_{[t_0, t]}), \gamma_{12} \circ \gamma_{2d}(\|d_2\|_{[t_0, t]}), \\ \max_{j \notin S_2} \max\{\gamma_{1j}, \gamma_{12} \circ \gamma_{2j}\}(\|x_j\|_{[t_0, t]})\}. \end{aligned} \quad (47)$$

By symmetry, there is class \mathcal{KL} function $\tilde{\beta}_2$ such that

$$\begin{aligned} \|x_2(t)\| &\leq \max\{\tilde{\beta}_2(\|x\|_\infty, t - t_0), \\ \gamma_{2d}(\|d_2\|_{[t_0, t]}), \gamma_{21} \circ \gamma_{1d}(\|d_1\|_{[t_0, t]}), \\ \max_{j \notin S_2} \max\{\gamma_{2j}, \gamma_{21} \circ \gamma_{1j}\}(\|x_j\|_{[t_0, t]})\}. \end{aligned} \quad (48)$$

Hence, we have shown that (42) holds for $\ell = 2$. Now assume (42) holds for some $\ell < n$. Recall that

$$\begin{aligned} \|x_{\ell+1}(t)\| &\leq \max\{\beta_{\ell+1}(\|x_{\ell+1}(t_0)\|, t - t_0), \\ \gamma_{\ell+1}(\|d_{\ell+1}\|_{[t_0, t]}), \max_{j \neq \ell+1} \gamma_{ij}(\|x_j\|_{[t_0, t]})\}. \end{aligned} \quad (49)$$

By using similar arguments towards the case of $\ell = 2$, one can show (42) holds for $\ell + 1$. Now we proceed to find a relation between $\|x\|_\infty$ and $\|d\|_\infty$. Because $\|x_i(t_0)\| \leq \|x(t_0)\|$, note that

$$\begin{aligned} \|x_i\|_\infty &\leq \max\{\beta_i(\|x(t_0)\|, 0), \gamma_{id}(\|d_i\|_{[t_0, t]}), \\ \max_{j \neq i} \gamma_{ij}(\|x_j\|_\infty)\}. \end{aligned}$$

Similar to (42), one can show by induction that there are class \mathcal{K} functions ρ_i and ρ_{id} such that

$$\|x_i\|_\infty \leq \max\{\rho_i(\|x(t_0)\|), \rho_{id}(\|d_i\|_{[t_0, t]})\}. \quad (50)$$

The combination of (50) and (42) achieves the desired result. \blacksquare

Now proceed with the proof that function $\beta(x, t) = |\mathcal{V}| \sum_{i \in \mathcal{V}} \beta_i(|\mathcal{V}| \sum_{k \in \mathcal{V}} \beta_k(x, 0), \frac{t}{(2\mathcal{L})^{|\mathcal{V}|-1}})$ is a candidate of class \mathcal{KL} function β in (33). We first find candidates of functions $\tilde{\beta}_i^{[\ell-1]}$ in (42) and ρ_i in (50) and then combine them together. Note that by substituting (45) into (43), we have equation (46). Consider class \mathcal{KL} functions in equation (46):

$$\begin{aligned} \|x_1(t_0 + T)\| &\leq \max\{\beta_1(\|x\|_\infty, \frac{1}{2\mathcal{L}}T), \gamma_{12} \circ \beta_2(\|x\|_\infty, \frac{1}{\mathcal{L}}T)\} \\ &\leq \max\{\beta_1(\|x\|_\infty, \frac{1}{2\mathcal{L}}T) + \beta_2(\|x\|_\infty, \frac{1}{2\mathcal{L}}T)\}. \end{aligned}$$

This implies that, in (47), $\tilde{\beta}_1(x, t) = \sum_{k=1}^2 \beta_k(x, \frac{t}{2\mathcal{L}})$ is a \mathcal{KL} function candidate. Likewise, in (42),

$$\tilde{\beta}_i^{[\ell-1]}(x, t) = \sum_{k=1}^{\ell} \beta_k(x, \frac{t}{(2\mathcal{L})^{\ell-1}}) \quad (51)$$

is a \mathcal{KL} function candidate for $\forall i \in S_{\ell}$ because we conduct $\ell - 1$ times of the substitutions. In a similar way, one can show that, in (50),

$$\rho_i(x) = \sum_{k=1}^{\ell} \beta_k(x, 0) \quad (52)$$

is a class \mathcal{K} function candidate for $\forall i \in S_{\ell}$. Now we proceed to find a relation between $\tilde{\beta}_i^{[\ell-1]}$ and ρ_i when $S_{\ell} = \mathcal{V}$. With equation (50),

$$\begin{aligned} \|x\|_{\infty} &\leq \sum_{i \in \mathcal{V}} \|x_i\|_{\infty} \\ &\leq |\mathcal{V}| \max_{i \in \mathcal{V}} \{\rho_i(\|x(t_0)\|), \rho_{id}(\|d_i\|_{[t_0, t]})\}. \end{aligned} \quad (53)$$

By combining (42) and (53),

$$\begin{aligned} \|x_i(t)\| &\leq \max\{\tilde{\beta}_i^{[|\mathcal{V}|-1]}(|\mathcal{V}| \max_{k \in \mathcal{V}} \rho_k(\|x(t_0)\|), t - t_0), \\ &\quad \gamma_i^{[\ell-1]}(\|d\|_{[t_0, t]})\}. \end{aligned}$$

This implies that

$$\beta(x, t) = |\mathcal{V}| \max_{i \in \mathcal{V}} \tilde{\beta}_i^{[|\mathcal{V}|-1]}(|\mathcal{V}| \max_{k \in \mathcal{V}} \rho_k(x), t) \quad (54)$$

is one of the class \mathcal{KL} function candidates. By applying (51) and (52) to (54), we have the result. \blacksquare

Remark 7.1 If functions $\beta_i(\cdot)$ in (32) for $\forall i \in \mathcal{V}$ are $\beta_i(x, t) = a_i^{-p_i(t)} r_i(x)$, then $\beta(\cdot)$ in (33) is also in the same form: $\beta(x, t) = a^{-p(t)} r(x)$ where $a, a_i > 0$ are constants, $p(t), p_i(t)$ are increasing functions without bound and $r(x), r_i(x)$ are class \mathcal{K} functions. \blacksquare

Remark 7.1 indicates that if functions $\beta_i(\cdot)$ are exponential functions, then $\beta(\cdot)$ is also an exponential function.

References

- [1] T. Ackermann. *Wind power in power systems*, volume 140. Wiley Online Library, 2005.
- [2] F. Alvarado. The stability of power system markets. *Power Systems, IEEE Transactions on*, 14(2):505–511, 1999.
- [3] F.L. Alvarado, J. Meng, C.L. DeMarco, and W.S. Mota. Stability analysis of interconnected power systems coupled with market dynamics. *IEEE Transactions on power systems*, 16(4):695–701, 2001.
- [4] A. Annaswamy, D. Callaway, J. Chow, C. DeMarco, D. Hill, P. Khargonekar, A. Rantzer, and J. Stoustrup. Guest editorial special section on control theory and technology. *IEEE Transactions on smart grid*, 5(4):2031–2032, 2014.
- [5] J. Apt. The spectrum of power from wind turbines. *Journal of Power Sources*, 169(2):369–374, 2007.
- [6] H. Bevrani, Y. Mitani, K. Tsuji, and H. Bevrani. Bilateral based robust load frequency control. *Energy conversion and management*, 46(7):1129–1146, 2005.
- [7] R. Bhatia and P. Rosenthal. How and why to solve the operator equation $ax - xb = y$. *Bulletin of the London Mathematical Society*, 29(01):1–21, 1997.
- [8] M. Bürger, C. De Persis, and S. Trip. An internal model approach to (optimal) frequency regulation in power grids. *arXiv preprint*, 2014.
- [9] W. Chiu, H. Sun, and H. V. Poor. Energy imbalance management using a robust pricing scheme. *Smart Grid, IEEE Transactions on*, 4(2):896–904, 2013.
- [10] N. Cohn. Some aspects of tie-line bias control on interconnected power systems. *IEEE Transactions on Power Apparatus and Systems*, pages 1415–1436, 1956.
- [11] R. D’Andrea and G. E. Dullerud. Distributed control design for spatially interconnected systems. *Automatic Control, IEEE Transactions on*, 48(9):1478–1495, 2003.
- [12] G. E. Dullerud and R. D’Andrea. Distributed control of heterogeneous systems. *Automatic Control, IEEE Transactions on*, 49(12):2113–2128, 2004.
- [13] A. M. Foley, P. G. Leahy, A. Marvuglia, and E. J. McKeogh. Current methods and advances in forecasting of wind power generation. *Renewable Energy*, 37(1):1–8, 2012.
- [14] B.A. Francis and W.M. Wonham. The internal model principle of control theory. *Automatica*, 12(5):457–465, 1976.
- [15] D. Gautam, V. Vittal, and T. Harbour. Impact of increased penetration of dfiig-based wind turbine generators on transient and small signal stability of power systems. *Power Systems, IEEE Transactions on*, 24(3):1426–1434, 2009.
- [16] L. Guo, Y. Zhang, and C. S. Wang. A new battery energy storage system control method based on soc and variable filter time constant. In *Innovative Smart Grid Technologies (ISGT), 2012 IEEE PES*, pages 1–7. IEEE, 2012.
- [17] M. D. Ilic, L. Xie, U. A. Khan, and J. M. F. Moura. Modeling of future cyber-physical energy systems for distributed sensing and control. *IEEE Transactions on Systems, Man, and Cybernetics-Part A: Systems and Humans*, 4(40):825–838, 2010.
- [18] M.D. Ilic, Y. Makarov, and D. Hawkins. Operations of electric power systems with high penetration of wind power: Risks and possible solutions. *IEEE Power Engineering Society General Meeting*, pages 1 – 4, 2007.
- [19] A. Isidori and C. Byrnes. Output regulation of nonlinear systems. *Automatic Control, IEEE Transactions on*, 35(2):131–140, 1990.
- [20] G. Karmiris and T. Tengnr. Control method evaluation for battery energy storage system utilized in renewable smoothing. *Industrial Electronics Society, IECON 2013-39th Annual Conference of the IEEE*, pages 1566–1570, 2013.
- [21] T.M. Keep, F.E. Sifuentes, D.M. Auslander, and D.S. Callaway. Using load switches to control aggregated electricity demand for load following and regulation. In *Power and Energy Society General Meeting, 2011 IEEE*, pages 1–7. IEEE, 2011.

- [22] H.K. Khalil. *Nonlinear Systems*. Upper Saddle River: Prentice hall, 2002.
- [23] H. Kim and M. Zhu. Distributed robust frequency regulation of smart power grid with renewable integration. In *American Control Conference*, pages 2347–2352, Chicago, IL, Jul 2015.
- [24] M. Krstic, I. Kanellakopoulos, and P. Kokotovic. *Nonlinear and Adaptive Control Design*. John Wiley and Sons, 1995.
- [25] P. Kumar and D.P. Kothari. Recent philosophies of automatic generation control strategies in power systems. *Power Systems, IEEE Transactions on*, 20(1):346–357, 2005.
- [26] P. Kundur, N.J. Balu, and M.G. Lauby. *Power system stability and control*. McGraw-Hill, 1994.
- [27] G. Lalor, A. Mullane, and M. O’Malley. Frequency control and wind turbine technologies. *Power Systems, IEEE Transactions on*, 20(4):1905–1913, 2005.
- [28] C. K. Lee, N. R. Chaudhuri, B. Chaudhuri, and S. Yuen R. Hui. Droop control of distributed electric springs for stabilizing future power grid. *Smart Grid, IEEE Transactions on*, 4(3):1558–1566, 2013.
- [29] K.Y. Lim, Y. Wang, and R. Zhou. Robust decentralised load-frequency control of multi-area power systems. In *Generation, Transmission and Distribution, IEE Proceedings-*, volume 143, pages 377–386. IET, 1996.
- [30] C. Lu, C. Liu, and C. Wu. Effect of battery energy storage system on load frequency control considering governor deadband and generation rate constraint. *Energy Conversion, IEEE Transactions on*, 10(3):555–561, 1995.
- [31] N. Lu and D.J. Hammerstrom. Design considerations for frequency responsive grid friendly TM appliances. In *Transmission and Distribution Conference and Exhibition, 2005/2006 IEEE PES*, pages 647–652. IEEE, 2006.
- [32] J.F. Manwell, J.G. McGowan, and A.L. Rogers. *Wind energy explained: theory, design and application*. John Wiley and Sons Ltd, 2010.
- [33] L. D. Marinovici, J. Lian, K. Kalsi, P. Du, and M. Elizondo. Distributed hierarchical control architecture for transient dynamics improvement in power systems. *Power Systems, IEEE Transactions on*, 28(3):3065–3074, 2013.
- [34] J. M. Mauricio, A. Marano, A. Gómez-Expósito, and J. M. Ramos. Frequency regulation contribution through variable-speed wind energy conversion systems. *Power Systems, IEEE Transactions on*, 24(1):173–180, 2009.
- [35] C. Nichita, D. Luca, B. Dakyo, and E. Ceanga. Large band simulation of the wind speed for real time wind turbine simulators. *IEEE Transactions on energy conversion*, 17(4):523–529, 2002.
- [36] The U.S. Department of Energy. The smart grid: an introduction.
- [37] M. A Ortega-Vazquez and D. S. Kirschen. Estimating the spinning reserve requirements in systems with significant wind power generation penetration. *Power Systems, IEEE Transactions on*, 24(1):114–124, 2009.
- [38] B. Pal and B. Chaudhuri. *Robust control in power systems*. Springer Science & Business Media, 2006.
- [39] F.D. Priscoli, L. Marconi, and A. Isidori. A new approach to adaptive nonlinear regulation. *SIAM Journal on Control and Optimization*, 45(3):829–855, 2006.
- [40] Z. Qin, M. Liserre, F. Blaabjerg, and H. Wang. Energy storage system by means of improved thermal performance of a 3 MW grid side wind power converter. In *Industrial Electronics Society, IECON 2013-39th Annual Conference of the IEEE*, pages 736–742. IEEE, 2013.
- [41] G. Ray, A.N. Prasad, and G.D. Prasad. A new approach to the design of robust load-frequency controller for large scale power systems. *Electric power systems research*, 51(1):13–22, 1999.
- [42] Renewables REN21. Global status report, Paris, REN21 Secretariat, 2014, 2014.
- [43] IEEE Report. Dynamic models for steam and hydro turbines in power system studies. *Power Apparatus and Systems, IEEE Transactions on*, (6):1904–1915, 1973.
- [44] G. Rogers. *Power system oscillations*. Springer Science & Business Media, 2012.
- [45] F.C. Schweppe, R.D. Tabors, J.L. Kirtley Jr, H.R. Outhred, F.H. Pickel, and A.J. Cox. Homeostatic utility control. *Power Apparatus and Systems, IEEE Transactions on*, (3):1151–1163, 1980.
- [46] A. Serrani, A. Isidori, and L. Marconi. Semi-global nonlinear output regulation with adaptive internal model. *Automatic Control, IEEE Transactions on*, 46(8):1178–1194, 2001.
- [47] H. Shayeghi. A robust decentralized power system load frequency control. *Journal of Electrical Engineering*, 59(6):281–293, 2008.
- [48] D. D. Siljak, D. M. Stipanovic, and A. I. Zecevic. Robust decentralized turbine/governor control using linear matrix inequalities. *IEEE Transactions on Power Systems*, 17(3):715–722, 2002.
- [49] J. G. Sloopweg and W. L. Kling. The impact of large scale wind power generation on power system oscillations. *Electric Power Systems Research*, 67(1):9–20, 2003.
- [50] M. Soberanis and W. Mérida. Regarding the influence of the van der hoven spectrum on wind energy applications in the meteorological mesoscale and microscale. *Renewable Energy*, 81:286–292, 2015.
- [51] E. Sontag. Smooth stabilization implies coprime factorization. *Automatic Control, IEEE Transactions on*, 34(4):435–443, 1989.
- [52] E. D. Sontag and Y. Wang. On characterizations of the input-to-state stability property. *Systems & Control Letters*, 24(5):351–359, 1995.
- [53] N. Srebro. *Learning with matrix factorizations*. PhD thesis, Massachusetts Institute of Technology, 2004.
- [54] G. Strbac. Demand side management: Benefits and challenges. *Energy policy*, 36(12):4419–4426, 2008.
- [55] A. Uehara, A. Pratap, T. Goya, T. Senjyu, A. Yona, N. Urasaki, and T. Funabashi. A coordinated control method to smooth wind power fluctuations of a pmsg-based wecs. *Energy Conversion, IEEE Transactions on*, 26(2):550–558, 2011.
- [56] I. Van der Hoven. Power spectrum of horizontal wind speed in the frequency range from 0.0007 to 900 cycles per hour. *Journal of Meteorology*, 14(2):160–164, 1957.
- [57] P. Whittle. The risk-sensitive certainty equivalence principle. *Journal of Applied Probability*, pages 383–388, 1986.
- [58] A.J. Wood and B.F. Wollenberg. *Power Generation Operation and Control*. New York: Wiley, 1996.
- [59] F.F. Wu, K. Moslehi, and A. Bose. Power system control centers: Past, present, and future. *Proceedings of the IEEE*, 93(11):1890–1908, 2005.
- [60] L. Xie, P.M.S. Carvalho, L.A.F.M. Ferreira, J. Liu, B.H. Krogh, N.Popli, and M.D. Ilic. Wind integration in power systems: Operational challenges and possible solutions. *Proceedings of the IEEE*, 99(1):214–232, 2011.

- [61] K. Yoshimoto, T. Nanahara, and G. Koshimizu. New control method for regulating state-of-charge of a battery in hybrid wind power/battery energy storage system. In *Power Systems Conference and Exposition, 2006. PSCE'06. 2006 IEEE PES*, pages 1244–1251. IEEE, 2006.
- [62] C. Zhao, U. Topcu, N. Li, and S.H. Low. Design and stability of load-side primary frequency control in power systems. *Automatic Control, IEEE Transactions on*, 59(5):1177–1189, 2014.
- [63] M. Zhu and J. Huang. Small gain theorem with restrictions for uncertain time-varying nonlinear systems. *Communication in Information and Systems*, 6(2):115–136, 2006.